

## Measurement of the Direct Photon Momentum Spectrum in $\Upsilon(1S)$ , $\Upsilon(2S)$ , and $\Upsilon(3S)$ Decays\*

D. Besson,<sup>1</sup> S. Henderson,<sup>1</sup> T. K. Pedlar,<sup>2</sup> D. Cronin-Hennessy,<sup>3</sup> K. Y. Gao,<sup>3</sup>  
 D. T. Gong,<sup>3</sup> J. Hietala,<sup>3</sup> Y. Kubota,<sup>3</sup> T. Klein,<sup>3</sup> B. W. Lang,<sup>3</sup> S. Z. Li,<sup>3</sup> R. Poling,<sup>3</sup>  
 A. W. Scott,<sup>3</sup> A. Smith,<sup>3</sup> S. Dobbs,<sup>4</sup> Z. Metreveli,<sup>4</sup> K. K. Seth,<sup>4</sup> A. Tomaradze,<sup>4</sup>  
 P. Zweber,<sup>4</sup> J. Ernst,<sup>5</sup> K. Arms,<sup>6</sup> H. Severini,<sup>7</sup> D. M. Asner,<sup>8</sup> S. A. Dytman,<sup>8</sup> W. Love,<sup>8</sup>  
 S. Mehrabyan,<sup>8</sup> J. A. Mueller,<sup>8</sup> V. Savinov,<sup>8</sup> Z. Li,<sup>9</sup> A. Lopez,<sup>9</sup> H. Mendez,<sup>9</sup> J. Ramirez,<sup>9</sup>  
 G. S. Huang,<sup>10</sup> D. H. Miller,<sup>10</sup> V. Pavlunin,<sup>10</sup> B. Sanghi,<sup>10</sup> I. P. J. Shipsey,<sup>10</sup>  
 G. S. Adams,<sup>11</sup> M. Cravey,<sup>11</sup> J. P. Cummings,<sup>11</sup> I. Danko,<sup>11</sup> J. Napolitano,<sup>11</sup>  
 Q. He,<sup>12</sup> H. Muramatsu,<sup>12</sup> C. S. Park,<sup>12</sup> E. H. Thorndike,<sup>12</sup> T. E. Coan,<sup>13</sup>  
 Y. S. Gao,<sup>13</sup> F. Liu,<sup>13</sup> R. Stroynowski,<sup>13</sup> M. Artuso,<sup>14</sup> C. Boulahouache,<sup>14</sup> S. Blusk,<sup>14</sup>  
 J. Butt,<sup>14</sup> O. Dorjkhaidav,<sup>14</sup> J. Li,<sup>14</sup> N. Mena,<sup>14</sup> G. Moneti,<sup>14</sup> R. Mountain,<sup>14</sup>  
 R. Nandakumar,<sup>14</sup> K. Randrianarivony,<sup>14</sup> R. Redjimi,<sup>14</sup> R. Sia,<sup>14</sup> T. Skwarnicki,<sup>14</sup>  
 S. Stone,<sup>14</sup> J. C. Wang,<sup>14</sup> K. Zhang,<sup>14</sup> S. E. Csorna,<sup>15</sup> G. Bonvicini,<sup>16</sup> D. Cinabro,<sup>16</sup>  
 M. Dubrovin,<sup>16</sup> A. Bornheim,<sup>17</sup> S. P. Pappas,<sup>17</sup> A. J. Weinstein,<sup>17</sup> R. A. Briere,<sup>18</sup>  
 G. P. Chen,<sup>18</sup> J. Chen,<sup>18</sup> T. Ferguson,<sup>18</sup> G. Tatishvili,<sup>18</sup> H. Vogel,<sup>18</sup> M. E. Watkins,<sup>18</sup>  
 J. L. Rosner,<sup>19</sup> N. E. Adam,<sup>20</sup> J. P. Alexander,<sup>20</sup> K. Berkelman,<sup>20</sup> D. G. Cassel,<sup>20</sup>  
 V. Crede,<sup>20</sup> J. E. Duboscq,<sup>20</sup> K. M. Ecklund,<sup>20</sup> R. Ehrlich,<sup>20</sup> L. Fields,<sup>20</sup> R. S. Galik,<sup>20</sup>  
 L. Gibbons,<sup>20</sup> B. Gittelmann,<sup>20</sup> R. Gray,<sup>20</sup> S. W. Gray,<sup>20</sup> D. L. Hartill,<sup>20</sup> B. K. Heltsley,<sup>20</sup>  
 D. Hertz,<sup>20</sup> C. D. Jones,<sup>20</sup> J. Kandaswamy,<sup>20</sup> D. L. Kreinick,<sup>20</sup> V. E. Kuznetsov,<sup>20</sup>  
 H. Mahlke-Krüger,<sup>20</sup> T. O. Meyer,<sup>20</sup> P. U. E. Onyisi,<sup>20</sup> J. R. Patterson,<sup>20</sup> D. Peterson,<sup>20</sup>  
 E. A. Phillips,<sup>20</sup> J. Pivarski,<sup>20</sup> D. Riley,<sup>20</sup> A. Ryd,<sup>20</sup> A. J. Sadoff,<sup>20</sup> H. Schwarthoff,<sup>20</sup>  
 X. Shi,<sup>20</sup> M. R. Shepherd,<sup>20</sup> S. Stroiney,<sup>20</sup> W. M. Sun,<sup>20</sup> D. Urner,<sup>20</sup> T. Wilksen,<sup>20</sup>  
 K. M. Weaver,<sup>20</sup> M. Weinberger,<sup>20</sup> S. B. Athar,<sup>21</sup> P. Avery,<sup>21</sup> L. Brevva-Newell,<sup>21</sup>  
 R. Patel,<sup>21</sup> V. Potlia,<sup>21</sup> H. Stoeck,<sup>21</sup> J. Yelton,<sup>21</sup> P. Rubin,<sup>22</sup> C. Cawfield,<sup>23</sup>  
 B. I. Eisenstein,<sup>23</sup> G. D. Gollin,<sup>23</sup> I. Karliner,<sup>23</sup> D. Kim,<sup>23</sup> N. Lowrey,<sup>23</sup> P. Naik,<sup>23</sup>  
 C. Sedlack,<sup>23</sup> M. Selen,<sup>23</sup> E. J. White,<sup>23</sup> J. Williams,<sup>23</sup> J. Wiss,<sup>23</sup> and K. W. Edwards<sup>24</sup>

(CLEO Collaboration)

<sup>1</sup>University of Kansas, Lawrence, Kansas 66045

<sup>2</sup>Luther College, Decorah, Iowa 52101

<sup>3</sup>University of Minnesota, Minneapolis, Minnesota 55455

<sup>4</sup>Northwestern University, Evanston, Illinois 60208

<sup>5</sup>State University of New York at Albany, Albany, New York 12222

<sup>6</sup>Ohio State University, Columbus, Ohio 43210

<sup>7</sup>University of Oklahoma, Norman, Oklahoma 73019

<sup>8</sup>University of Pittsburgh, Pittsburgh, Pennsylvania 15260

<sup>9</sup>University of Puerto Rico, Mayaguez, Puerto Rico 00681

<sup>10</sup>Purdue University, West Lafayette, Indiana 47907

<sup>11</sup>Rensselaer Polytechnic Institute, Troy, New York 12180

<sup>12</sup>University of Rochester, Rochester, New York 14627

<sup>13</sup>Southern Methodist University, Dallas, Texas 75275

<sup>14</sup>Syracuse University, Syracuse, New York 13244

<sup>15</sup>Vanderbilt University, Nashville, Tennessee 37235

<sup>16</sup>Wayne State University, Detroit, Michigan 48202

<sup>17</sup>California Institute of Technology, Pasadena, California 91125

<sup>18</sup>Carnegie Mellon University, Pittsburgh, Pennsylvania 15213

<sup>19</sup>Enrico Fermi Institute, University of Chicago, Chicago, Illinois 60637

<sup>20</sup>Cornell University, Ithaca, New York 14853

<sup>21</sup>University of Florida, Gainesville, Florida 32611

<sup>22</sup>George Mason University, Fairfax, Virginia 22030

<sup>23</sup>University of Illinois, Urbana-Champaign, Illinois 61801

<sup>24</sup>Carleton University, Ottawa, Ontario, Canada K1S 5B6  
and the Institute of Particle Physics, Canada

(Dated: June 30, 2005)

## Abstract

Using data taken with the CLEO III detector at the Cornell Electron Storage Ring, we have investigated the direct photon spectrum in the decays  $\Upsilon(1S) \rightarrow \gamma gg$ ,  $\Upsilon(2S) \rightarrow \gamma gg$ ,  $\Upsilon(3S) \rightarrow \gamma gg$ . The latter two of these are first observations. Our measurement procedures differ from previous ones in the following ways: a) background estimates (primarily from  $\pi^0$  decays) are based on isospin symmetry rather than an explicit determination of the  $\pi^0$  spectrum, which permits measurement of the  $\Upsilon(2S)$  and  $\Upsilon(3S)$  direct photon spectra without having to explicitly correct for  $\pi^0$  backgrounds from, e.g.,  $\chi_b$  states, b) we estimate the branching fractions with a parametrized functional form (exponential) used for the background, c) we use the high-statistics sample of  $\Upsilon(2S) \rightarrow \pi\pi\Upsilon(1S)$  to obtain a tagged-sample of  $\Upsilon(1S) \rightarrow \gamma + X$  events, for which there are no QED backgrounds. We determine preliminary values for the ratio of the inclusive direct photon decay rate to that of the dominant three-gluon decay  $\Upsilon \rightarrow ggg$  ( $R_\gamma = B(gg\gamma)/B(ggg)$ ) to be:  $R_\gamma(1S) = 2.80 \pm 0.007 \pm 0.24 \pm 0.14$ ,  $R_\gamma(2S) = 3.45 \pm 0.03 \pm 0.58 \pm 0.18$ , and  $R_\gamma(3S) = 2.89 \pm 0.03 \pm 0.38 \pm 0.03$ , where the errors shown are statistical, systematic, and theoretical model-dependence, respectively. Given a value of  $Q^2$ , one can estimate a value for the strong coupling constant  $\alpha_s(Q^2)$  from  $R_\gamma$ .

---

\*Submitted to the XXII International Symposium on Lepton and Photon Interactions at High Energies, June 30-July 5, 2005, Uppsala, Sweden

## Introduction

According to the Zweig rule, the preferred decay mode for an  $\Upsilon$  meson would be through the production of a  $B\bar{B}$  meson pair. For resonances below the  $\Upsilon(4S)$  however, this is not energetically possible. Thus the decay of the  $\Upsilon(1S)$  meson must proceed through Zweig-suppressed channels. Since the charge conjugation of the  $\Upsilon$  resonances is  $C=-1$ , the three lowest order decay modes of the  $\Upsilon(1S)$  meson are the three-gluon ( $ggg$ ), single photon (vacuum polarization) QED decay  $\Upsilon \rightarrow q\bar{q}$ , and two gluon plus single photon ( $gg\gamma$ ) modes. For the  $\Upsilon(2S)$  and  $\Upsilon(3S)$  resonances, direct radiative transitions, both electromagnetic and hadronic, compete with these annihilation modes. Since  $\Gamma_{ggg} \propto \alpha_s^3$  and  $\Gamma_{gg\gamma} \propto \alpha_s^2\alpha_{em}$ , the ratio of the decay rates from these two processes[1]:

$$R_\gamma \equiv \frac{\Gamma_{gg\gamma}}{\Gamma_{ggg}} = \frac{N_{gg\gamma}}{N_{ggg}} = \frac{38}{5} q_b^2 \frac{\alpha_{em}}{\alpha_s} [1 + (2.2 \pm 0.8)\alpha_s/\pi] \quad (1)$$

In this expression, the bottom quark charge  $q_b = 1/3$ . Alternately, one can normalize to the well-measured dimuon channel and cancel the electromagnetic vertex:

$$\frac{\Gamma_{gg\gamma}}{\Gamma_{\mu\mu}} \propto \alpha_s^2 \quad (2)$$

In either case, one must define the value of  $Q^2$  appropriate for this process – although the value  $Q^2 \sim M_\Upsilon^2$  seems ‘natural’, the original prescription of Brodsky *et al.*[1] gave  $Q = 0.157M_{\Upsilon(1S)}$  for  $\Upsilon(1S) \rightarrow gg\gamma$ .

Theory prescribes the differential spectrum  $d^2N/dxd(\cos\theta)$  ( $x = p_\gamma/E_{beam}$ ,  $\cos\theta$  is the polar angle relative to the  $e^+e^-$  beam axis). The limited angular coverage of the high-resolution photon detection, as well as the large backgrounds at low momentum, due to decays of hadrons to photons, plus the large number of radiated final state ‘fragmentation’ photons in this regime limit our sensitivity to the region defined by  $|\cos\theta_z| < 0.7$  and  $x_\gamma > 0.4$ . We must therefore rely on models to efficiency-correct the observed spectrum and extrapolate into lower-momentum and larger polar angle regions.

Originally, the decay of the ground-state vector  $b\bar{b}$  bottomonium pair into three vectors (both  $\Upsilon \rightarrow ggg$  as well as  $\Upsilon \rightarrow gg\gamma$ ) was modeled in lowest-order QCD after similar QED decays of orthopositronium into three photons, leading to the expectation that the single photon spectrum should rise linearly with  $x$  to the kinematic limit ( $x \rightarrow 1$ ); phase space considerations lead to a slight enhancement exactly at the kinematic limit[2]. Koller and Walsh considered the angular spectrum in detail[5], demonstrating that as the momentum of the most energetic primary (photon or gluon) in  $\Upsilon \rightarrow \gamma gg$  or  $\Upsilon \rightarrow ggg$  approaches the beam energy, the event axis tends to increasingly align with the beam axis:  $x_\gamma \rightarrow 1$  corresponds to  $dN/d(\cos\theta) \rightarrow 1 + \cos^2\theta$ . Field[6] argued that  $x_\gamma = 1$  is non-physical, since it corresponds to a recoil  $gg$  system with zero invariant mass, while the recoil system must have enough mass to produce on-shell final state hadrons. Using a parton shower Monte Carlo technique which took into account the correlation of photon momentum with recoil hadronization phase space, Field predicted a significant softening of the lowest-order QCD predicted spectrum, with a resulting photon momentum distribution peaking at  $x_\gamma \sim 0.65$  rather than  $x \rightarrow 1$ . This result seemed in conflict with the extant CUSB[7] data, which indicated a spectrum more similar to the lowest-order QCD prediction. A subsequent measurement by CLEO-I[8], however, favored Field’s softened spectrum over lowest-order QCD, as well as a subsequent modification to lowest-order QCD which calculated corrections at

the endpoint[9] by summing leading logs of the form  $\ln(1-x)$ . Higher statistics measurements by Crystal Ball[10] as well as ARGUS[11] corroborated this softened photon spectrum.<sup>1</sup> The previous CLEO analysis (CLEO-II), based on  $\sim 1$  M  $\Upsilon(1S)$  events provided a high-statistics confirmation of a photon spectrum peaking at  $x_\gamma \sim 0.65$ , and were able to trace the direct photon momentum spectrum down to  $x_\gamma \approx 0.4$ ; at that momentum, the direct photon signal becomes less than 10% relative to the background, whereas the systematic errors on the background estimate in that momentum region are of order 10%, as well.<sup>2</sup> Contemporary with the CLEO-II analysis, Catani and Hautmann argued that in addition to the usual *direct* photon, *fragmentation* photons emitted from final-state light quarks down stream of the initial heavy quarkonia decay [12] (essentially final state radiation) will also contribute to the background-subtracted spectra for  $x_\gamma < 0.4$  and therefore (if not corrected for) lead to an over-estimate of the  $\Upsilon(1S) \rightarrow gg\gamma$  branching fraction.<sup>3</sup>

Hoodbhoy and Yusuf[13] also performed a rigorous calculation of the expected  $\Upsilon(1S) \rightarrow gg\gamma$  decay rate, by summing all the diagrams contributing to the direct photon final state and treating hard and soft contributions separately. Rather than assuming that the decay occurs via annihilation of two at-rest quarks, the authors smear the annihilation over a size of order  $1/m$ , with a corresponding non-zero velocity. Although their calculation results in some softening of the photon spectrum relative to the lowest-order QCD prediction, it is unable to entirely account for the softening observed in data, leading to the conclusion that final-state gluon interactions (largely incalculable) are, indeed, important particularly near the photon endpoint.

Fleming and Leibovich[14] considered the photon spectrum in three distinct momentum regions - at low momentum  $x_\gamma < 0.3$ , final-state radiation effects[12] (sometimes referred to as ‘fragmentation photons’) dominate. In the intermediate momentum regime ( $0.3 < x_\gamma < 0.7$ ), they applied the Operator Product Expansion (OPE) to the direct photon spectrum of  $\Upsilon$  decay, with power-counting rules prescribed by non-relativistic QCD, and retained only the lowest-order color singlet terms in  $v/c$ . In the highest-momentum regime ( $x_\gamma > 0.7$ ), a soft-collinear effective theory (SCET) for the light degrees of freedom combined with non-relativistic QCD for the heavy degrees of freedom, was used to obtain a prediction for the photon spectrum which qualitatively described the essential features of the CLEO-II data, despite peaking at a higher value of  $x_\gamma$  than data. The same approach was later applied by Fleming to decays of the type  $e^+e^- \rightarrow \psi + X$ , given the similarity to  $e^+e^- \rightarrow \Upsilon(1S) \rightarrow \gamma + X$ , but including the color-octet contributions to  $\psi$  production[15].

Very recently, Garcia and Soto (GS[16]) have also produced a parameterization of the expected photon momentum spectrum in the  $\Upsilon$  system. Following Fleming and Leibovich,

---

<sup>1</sup> It is important to note here that all these measurements assumed that the Koller-Walsh angular distribution was still applicable to the phenomenological Field model.

<sup>2</sup> We emphasize here that the previous CLEO-II analysis, in presenting their background-subtracted direct photon spectrum, showed only statistical errors, whereas the systematic errors in the region  $x < 0.4$  are considerably larger than those statistical errors. This is a point that was not made strongly enough in the past, encouraging various theoretical fragmentation models to be tested against our direct photon data at low  $x_\gamma$  values.

<sup>3</sup> Therefore, to properly measure  $\alpha_s$ , one must account for these additional photons, both in the shape of the spectrum, as well the QCD equations from which  $\alpha_s$  is extracted. Due to existing limitations in perturbative QCD however, Catani and Hautmann do not specify how to actually calculate  $\alpha_s$  from quarkonia decay, beyond the admonition to quote “generous” theoretical uncertainties.

they also remedy the inability of non-relativistic perturbative QCD (NRQCD) to model the endpoint region by combining NRQCD with Soft Collinear-Effective Theory, which allows calculation of the spectrum of the collinear gluons resulting as  $x_\gamma \rightarrow 1$ . They make their own calculation of the octet contributions (in both S- and P- partial waves) to the overall rate, obtaining a spectral shape prediction similar to Fleming and Leibovich (claimed to be reliable in the interval  $0.7 < x_\gamma < 0.95$ ), after adding color-octet, color-singlet, and fragmentation contributions. We have compared our results with their parameterization, as well.

In this analysis, we primarily employ the models by Field and Garcia-Soto for integration purposes. Although no predictions exist for direct photon decays of the  $\Upsilon(2S)$  and  $\Upsilon(3S)$  resonances, we nevertheless use these same models to determine total direct photon decay rates in the case of these higher resonances.

### Data Sets and Event Criteria

The CLEO III detector is a general purpose solenoidal magnet spectrometer and calorimeter. Elements of the detector, as well as performance characteristics, are described in detail elsewhere [17–19]. For photons in the central “barrel” region of the CsI electromagnetic calorimeter the energy resolution is given by

$$\frac{\sigma_E}{E}(\%) = \frac{0.35}{E^{0.75}} + 1.9 - 0.1E, \quad (3)$$

where  $E$  is the shower energy in GeV. The tracking system, RICH particle identification system, and calorimeter are all contained within a 1 Tesla superconducting coil.

The data used in this analysis were collected on the  $\Upsilon(1S)$  resonance, center-of-mass energy  $E_{cm} = 9.46$  GeV, the  $\Upsilon(2S)$  resonance, center-of-mass energy  $E_{cm} = 10.02$  GeV, and the  $\Upsilon(3S)$  resonance, center-of-mass energy  $E_{cm} = 10.36$  GeV. In order to check our background estimates, we used continuum (below the  $\Upsilon$  resonances) running. These data were collected below the  $\Upsilon(1S)$  resonance, center-of-mass energy  $9.431 \text{ GeV} < E_{cm} < 9.4342 \text{ GeV}$ , below the  $\Upsilon(2S)$  resonance, center-of-mass energy  $9.9956 \text{ GeV} < E_{cm} < 10.004 \text{ GeV}$ , below the  $\Upsilon(3S)$  resonance, center-of-mass energy  $10.3286 \text{ GeV} < E_{cm} < 10.3308 \text{ GeV}$  and below the  $\Upsilon(4S)$  resonance, center-of-mass energy  $10.41 \text{ GeV} < E_{cm} < 10.57$ .

To obtain a clean sample of hadronic events, we selected those events that had a minimum of four good charged tracks (to suppress contamination from QED events), a total visible energy greater than 15% of the total center-of-mass energy (to reduce contamination from two-photon events and beam-gas interactions), and an event vertex position consistent with the nominal  $e^+e^-$  collision point to within  $\pm 5$  cm along the  $e^+e^-$  axis ( $z$ ) and  $\pm 2$  cm in the transverse ( $r - \phi$ ) plane. We additionally veto events with a well-defined electron or muon, or consistent with a  $\tau\tau$  “1 vs. 3” topology. Our full data sample is summarized in Table I.

### Event Selection

To obtain  $R_\gamma$ , we had to determine the number of direct photon events and the number of three gluon events. Only photons from the barrel region ( $|\cos\theta_\gamma| < 0.7$ ) were considered. Photon candidates were required to be well separated from charged tracks and other photon candidates. The lateral shower shape was required to be consistent with that expected from a true photon. Photons produced in the decay of a highly energetic  $\pi^0$  would sometimes

DataSet	Resonance	$\mathcal{L}$	HadEvs	$\sigma_{obs}^{had}$ (nb)	EvtSel (raw)
1S-A	$\Upsilon(1S)$	6.717 /pb	128019	19.06	226746
1S-B	$\Upsilon(1S)$	675.496 /pb	12803279	18.95	15720815
1S-C	$\Upsilon(1S)$	453.852 /pb	8742850	19.26	10553140
2S-A	$\Upsilon(2S)$	472.311 /pb	4165745	8.82	6561803
2S-B	$\Upsilon(2S)$	6.426 /pb	55834	8.69	762086
2S-C	$\Upsilon(2S)$	206.920 /pb	1839390	8.89	2748240
2S-D	$\Upsilon(2S)$	257.920 /pb	2299910	8.92	2914640
2S-E	$\Upsilon(2S)$	295.556 /pb	2629250	8.90	3473320
3S-A	$\Upsilon(3S)$	391.814 /pb	2482170	6.34	3887570
3S-B	$\Upsilon(3S)$	620.908 /pb	3948690	6.36	5736980
3S-C	$\Upsilon(3S)$	187.889 /pb	1168980	6.22	2108220
1S-CO-A	$< \Upsilon(1S)$	148.214 /pb	485790	3.28	1619060
1S-CO-B	$< \Upsilon(1S)$	48.755 /pb	159959	3.28	260599
2S-CO-A	$< \Upsilon(2S)$	159.062 /pb	472071	2.97	6245050
2S-CO-B	$< \Upsilon(2S)$	110.070 /pb	326371	2.97	465939
2S-CO-C	$< \Upsilon(2S)$	33.433 /pb	99377	2.97	138898
2S-CO-D	$< \Upsilon(2S)$	61.659 /pb	183897	2.98	256185
2S-CO-E	$< \Upsilon(2S)$	46.195 /pb	137083	2.97	191205
3S-CO-A	$< \Upsilon(3S)$	47.744 /pb	135069	2.83	193749
3S-CO-B	$< \Upsilon(3S)$	80.591 /pb	226700	2.81	321169
3S-CO-C	$< \Upsilon(3S)$	32.944 /pb	91997	2.79	130021
4S-CO-A	$< \Upsilon(4S)$	219.159 /pb	594662	2.71	847875
4S-CO-B	$< \Upsilon(4S)$	569.869 /pb	1536020	2.70	2189720
4S-CO-C	$< \Upsilon(4S)$	276.755 /pb	753418	2.72	1073410
4S-CO-D	$< \Upsilon(4S)$	670.165 /pb	1815920	2.71	2587650
4S-CO-E	$< \Upsilon(4S)$	243.370 /pb	660883	2.72	941162
4S-CO-F	$< \Upsilon(4S)$	344.814 /pb	938454	2.72	1337990

TABLE I: Summary of data used in analysis. Different running periods are designated by capital roman letters. EvtSel denotes events analyzed on tape, HadEvs denotes the total number of events in each sample identified as hadronic by our event selection requirements, and  $\sigma$  is the corresponding observed hadronic crosssection for each data sample.

produce overlapping showers in the calorimeter, creating a so-called ‘merged’  $\pi^0$ . Two cuts were imposed to remove this background. First, any two photons which both have energies greater than 50 MeV and also have an opening angle  $\theta_{\gamma_1\gamma_2}$  such that  $\cos\theta_{\gamma_1\gamma_2} > 0.975$  are removed from candidacy as direct photons. Second, an effective invariant mass was determined from the energy distribution within a single electromagnetic shower. Showers whose effective invariant masses were consistent with those from merged  $\pi^0$ ’s were also rejected. After all photon selection requirements, the momentum-dependent photon-finding efficiency is shown in Figure 1.

The dominant backgrounds to the direct photon measurement are of two types: initial state radiation ( $x_\gamma > 0.65$ ) and the overwhelming number of background photons primarily from asymmetric  $\pi^0$  decays ( $x_\gamma < 0.65$ ), resulting in two, spatially well-separated daughter photons.

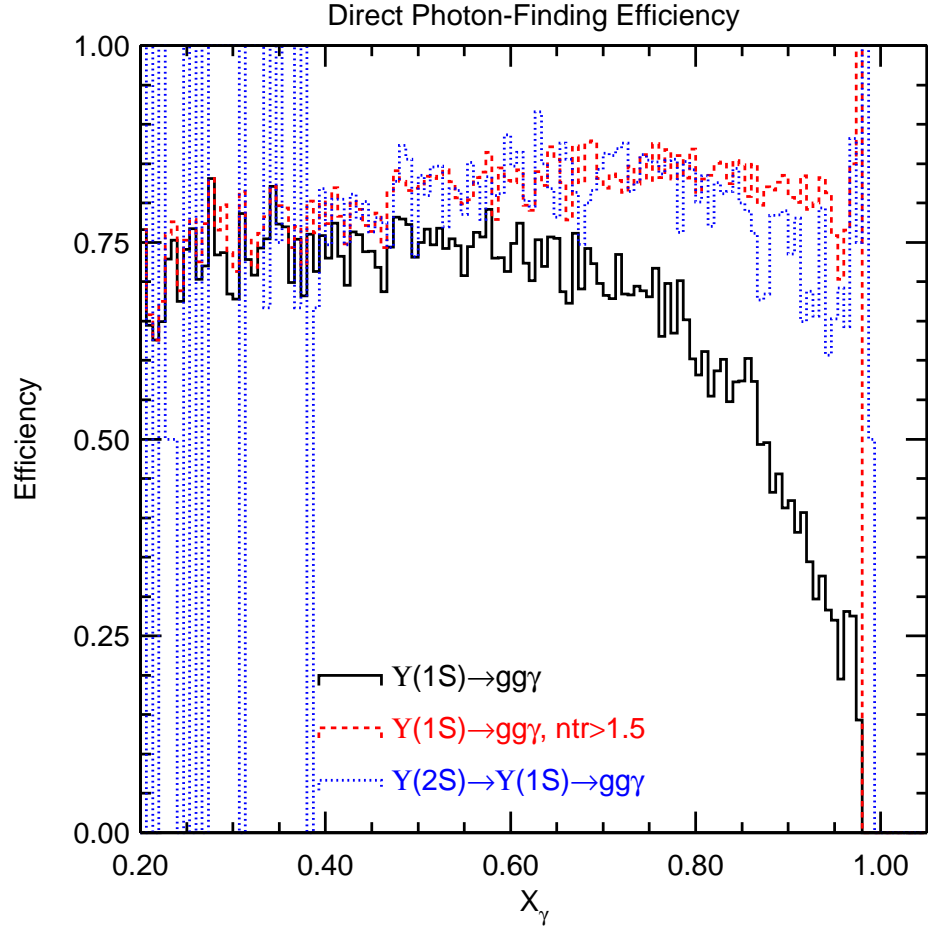


FIG. 1: Direct photon-finding efficiency for: a)  $\Upsilon(1S) \rightarrow \gamma gg$  using our default photon selection requirements and our default charged multiplicity requirement of  $\geq 4$  charged tracks observed in a candidate event (black, solid), b)  $\Upsilon(1S) \rightarrow \gamma gg$  showing the efficiency if the multiplicity requirement was relaxed to  $\geq 2$  charged tracks (red, dashed), and c) the photon-finding efficiency for finding an  $\Upsilon(1S)$  direct-photon daughter, for  $\Upsilon(1S)$  produced in  $\Upsilon(2S)$  dipion decays (blue, dashed, and discussed later in this document). Efficiencies are derived from full GEANT-based detector simulations.

If our Monte Carlo generator were sufficiently accurate, of course, we could use the Monte Carlo simulation itself to generate the expected background to the direct photon signal, including all background sources. We have compared the expected neutral spectrum with data (based on the JETSET 7.4 event generator plus a GEANT-based CLEO-III detector response simulation) for continuum events at  $ECM = 10.55$  GeV. We observe fair, but not excellent agreement between the two, motivating a data-driven estimate of the background to the direct photon signal. To model the production of  $\pi^0$  daughter photons, we took advantage of the similar kinematic distributions expected between charged and neutral pions, as dictated by isospin symmetry. Although isospin conservation will break down in the low-energy regime (where, e.g., the neutral vs. charged pion mass differences and contributions from weak decays may become important), at the high-energy end of the spectrum, we expect isospin to be reliable, so that there should be half as many neutral pions as charged pions. We stress here that this is true for three-gluon decays,  $\chi_b$  decays, continuum  $q\bar{q}$  events, etc. However, since: a) our charged  $\pi^\pm$  identification and tracking are slightly inefficient, b) charged kaons and protons may fake charged pions, and c) for low multiplicity events, it is more likely that an event with charged pions will pass our minimum charged-multiplicity requirement than an event with neutral pions, this ratio deviates slightly from 0.5, as a function of momentum. Figure 2 shows the Monte Carlo neutral to charged pion production ratio for continuum events taking into account such selection biases; we observe agreement with the 0.5 expectation to within 3%. In our analysis, we use this Monte Carlo simulation-derived efficiency, rather than the simple isospin expectation, to generate pseudo- $\pi^0$ 's. The deviation between this value and the simple isospin expectation is later incorporated into the systematic error.

These  $\pi^0$ 's are then subsequently decayed via phase space, and the resulting simulated photon spectrum (including our Monte Carlo-derived photon efficiency, and including the correlation between daughter photon momenta and the photon emission direction relative to the  $\pi^0$  flight direction in the lab) is then plotted. In addition to  $\pi^0$ 's, we also simulate  $\eta \rightarrow \gamma\gamma$ ,  $\omega \rightarrow \pi^0\gamma$ , and  $\eta' \rightarrow \gamma(\rho, \omega, \gamma)$  contributions, using previous measurements of these backgrounds in  $\Upsilon(1S)$  decays[20]. An estimate of the relative contribution of these various backgrounds to the observed continuum spectrum is shown in Figure 3.

We also studied the relative contribution to the inclusive spectrum from neutrons, anti-neutrons, and  $K_L^0$ 's. According to Monte Carlo simulations, the expected numbers of particles per hadronic event with  $|\cos(\theta)| < 0.7$ , and scaled momentum  $> 0.25$  (i.e., particles which could populate our signal region) are quite small. Figure 4 gives the yield per event, as a function of momentum, for  $K_L^0$  and anti-neutrons to populate our signal region. Contributions from  $K_L^0$  and neutrons are therefore neglected in the remainder of the analysis.

The performance of our photon-background estimator can be calibrated from data itself. Three cross-checks are presented below: a) the comparison between the absolutely normalized angular distribution of our simulated, pseudo-photons (“PP”, or “dkpigg” for “decay of  $\pi^0$  into  $\gamma\gamma$ ”)<sup>4</sup> versus continuum data (including a Monte Carlo-determined contribution from initial state radiation [“ISR”] (Figure 5)), b) a comparison of the absolute magnitude of the pseudo-photon momentum spectrum with continuum data (Figure 6), and c) a comparison of the reconstructed  $\pi^0$  mass peak (Figure 7) between our simulated photons and real data

---

<sup>4</sup> Note that there are two simulations referred to in this document – “simulated” PP photons refer to the pseudo-photons generated using identified charged pion tracks as inputs; “Monte Carlo” refers to the full JETSET+GEANT CLEO-III event+detector simulation.



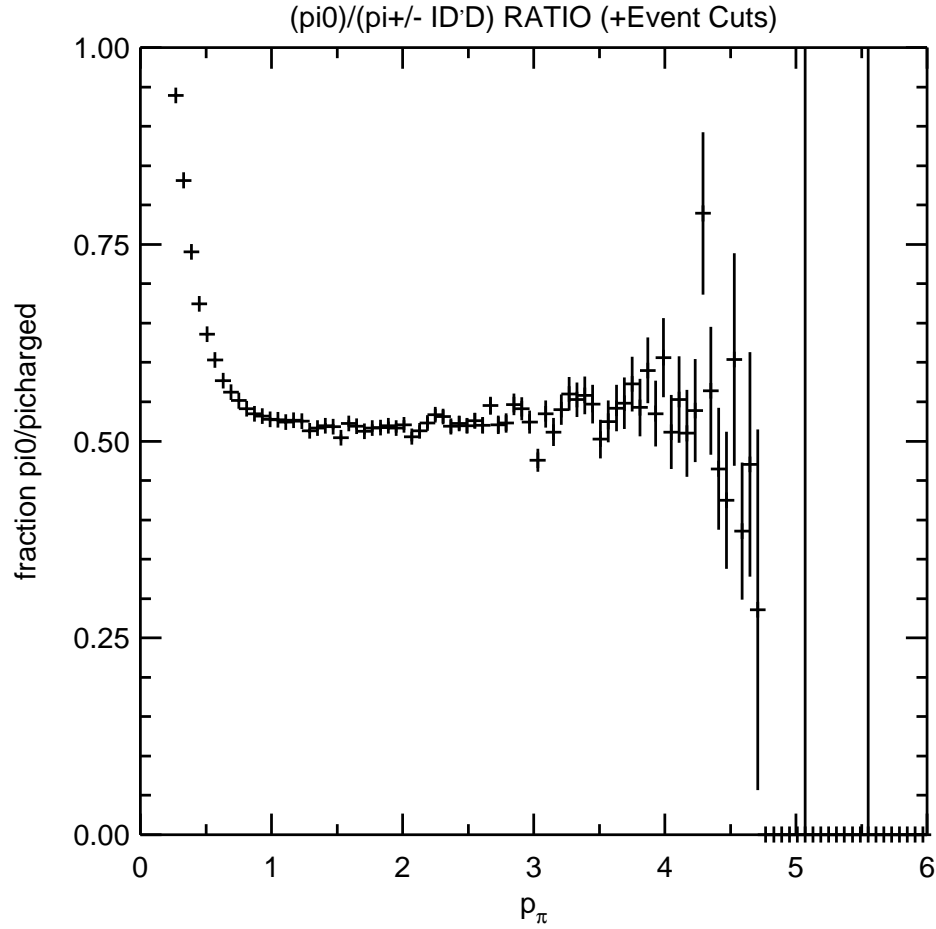


FIG. 2:  $\pi^0/(\pi^+ + \pi^-)$  ratio, as a function of charged pion momentum, including tracking efficiency, particle identification efficiency and event selection requirements (from Monte Carlo simulations). The loss of efficiency at large  $p_\pi$  is due to the bias introduced by the minimum charged-particle multiplicity requirement.

photons. All these checks show good agreement between simulation and data.

Other systematic checks of our data (photon yield per data set, comparison between the below- $\Upsilon(1S)$ , below- $\Upsilon(2S)$ , below- $\Upsilon(3S)$  and below- $\Upsilon(4S)$  continuum photon momentum spectra) indicate good internal consistency of all data sets considered.

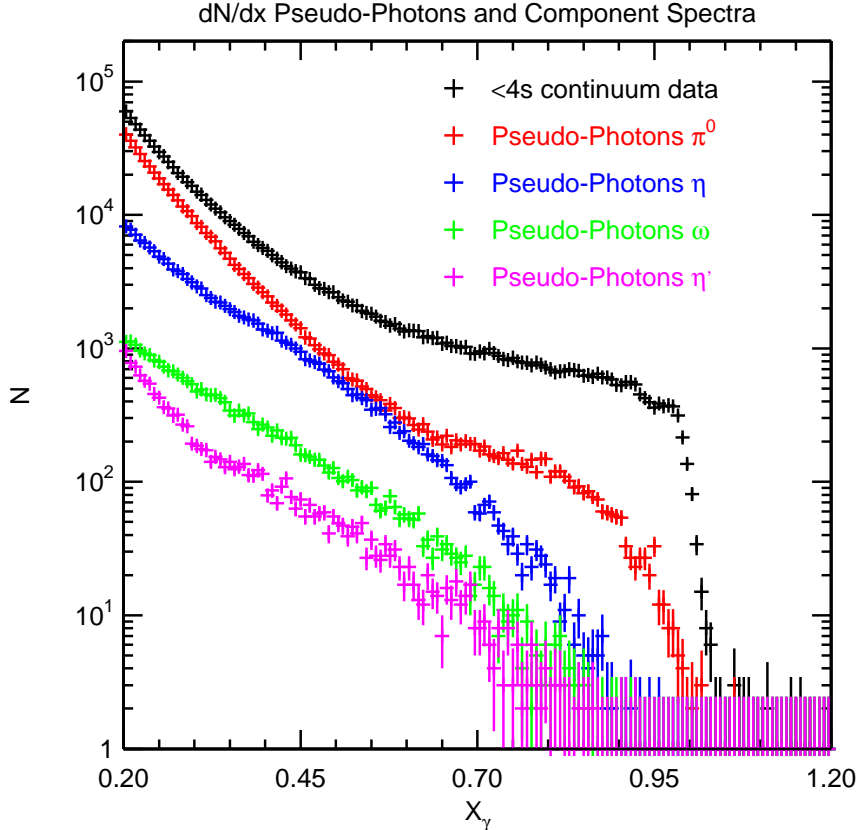


FIG. 3: Estimate of the momentum-dependent contribution from various background sources to the observed below- $\Upsilon(4S)$  inclusive photon spectrum. Initial state radiation contributions are not included.

### Signal Extraction

Three different methods were used to subtract pseudo-photons and obtain the  $\Upsilon(1S) \rightarrow gg\gamma$ ,  $\Upsilon(2S) \rightarrow gg\gamma$  and  $\Upsilon(3S) \rightarrow gg\gamma$  spectra. In the first, we generate pseudo-photons for all events taken at that center-of-mass energy. This procedure will account for background photons both from the continuum, as well as resonance events taken at a given center-of-mass energy, however it will not account for initial state radiation photons, which are subtracted using Monte Carlo simulations of continuum ISR events, normalized to our total event sample. Alternately, we explicitly subtract the measured photon spectrum from continuum events, which implicitly includes both ISR as well as hadronic-decay photons, and use the pseudo-photon spectrum to model only the resonant direct photon background due to hadronic decays (“CO ISR”). We additionally used an exponential parametrization of the background as a cross-check of our non-direct photon estimate.

Figure 8 shows the inclusive  $\Upsilon(1S)$  photon distribution with the different estimated

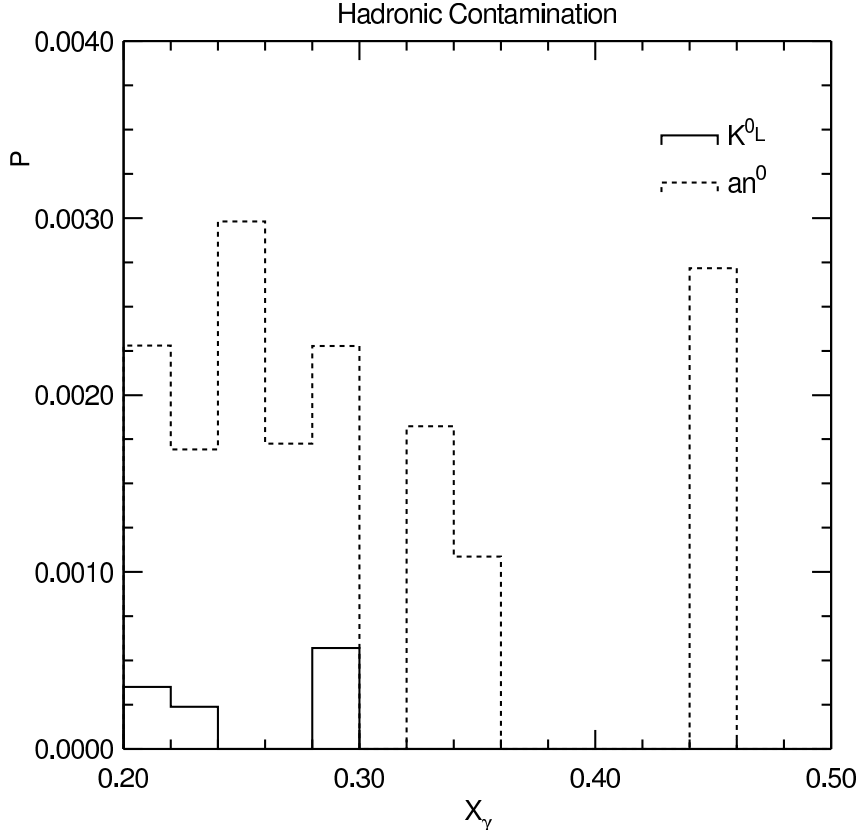


FIG. 4: Estimate of the momentum dependent percentage of showers produced by  $n^0$ 's,  $\bar{n}^0$ 's and  $K_L^0$ 's that passed our shower selection, based on a sample of 1 million MC continuum events.

background contributions (non-resonant radiative photons, and non-resonant and resonant hadronic decay photons) overlaid. After subtracting these sources, what remained of the inclusive  $\Upsilon(1S)$  spectrum was identified as the direct photon spectrum,  $\Upsilon(1S) \rightarrow gg\gamma$ . Figures 9 and 10 show the corresponding plots for the  $\Upsilon(2S)$  and  $\Upsilon(3S)$  data, and also indicate the magnitude of the cascade subtraction due to transitions of the type  $\Upsilon(2S) \rightarrow \Upsilon(1S)X$ ,  $\Upsilon(1S) \rightarrow \gamma gg$ . We use currently tabulated values for  $\Upsilon(2S) \rightarrow \Upsilon(1S)X$  to determine the magnitude of this correction; Monte Carlo simulations of the primary cascade processes, including  $\Upsilon(2S) \rightarrow \pi\pi\Upsilon(1S)$  (using a Yan[21] distribution for the dipion mass distribution) and  $\Upsilon(2S) \rightarrow \chi_b\gamma$ ;  $\chi_b \rightarrow \gamma\Upsilon(1S)$  are used to adjust the shape of our measured  $\Upsilon(1S) \rightarrow \gamma gg$  direct photon spectrum to that expected for the cascade subtraction in order to account for the shifted kinematic endpoint and Doppler smearing of the daughter  $\Upsilon(1S)$  direct photon spectrum.

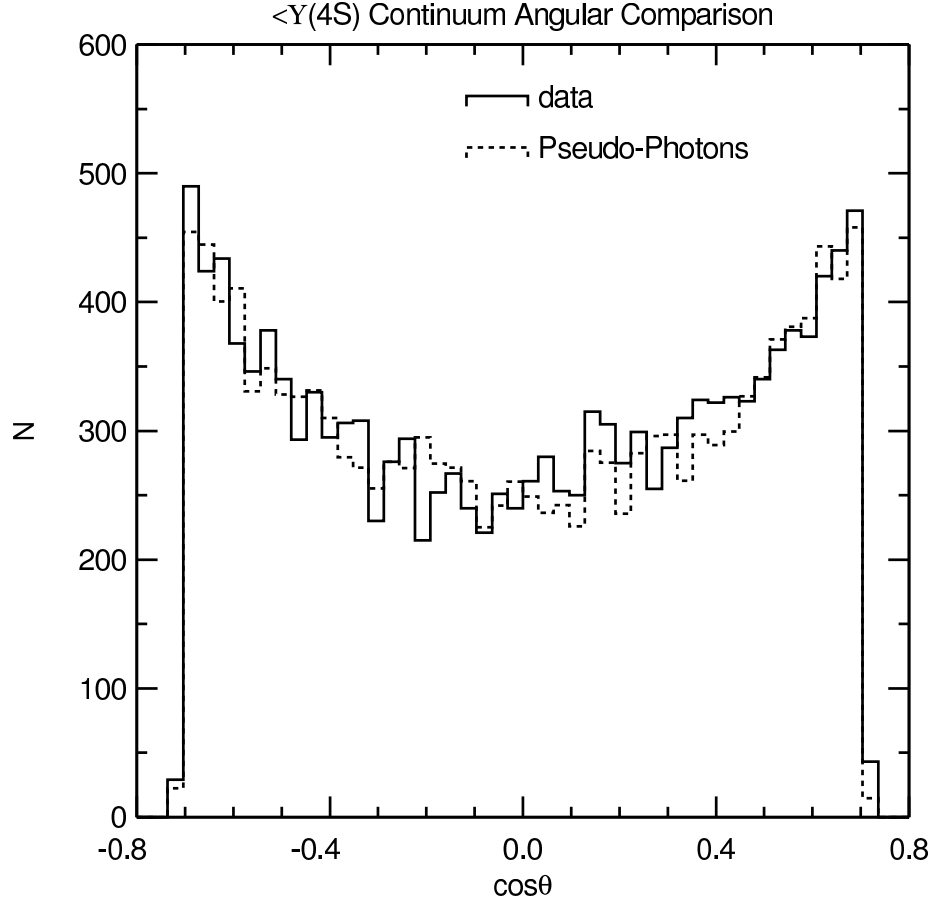


FIG. 5: Angular distribution of the inclusive photons from continuum data compared with our pseudo-photon estimate, based on isospin invariance, for showers with  $x_\gamma > 0.45$ , and including a Monte Carlo-based estimate of the ISR background. Normalization is absolute.

### Parametric estimate of background

Observing that the photon spectrum seems to describe an exponential outside the signal, we attempted to check our derived branching fractions against the branching fraction obtained when we simply fit the background to an exponential, in the momentum regime below the signal (comparing the results obtained from fitting  $0.2 < x_\gamma < 0.3$  to those obtained using  $0.3 < x_\gamma < 0.4$ ), and then extrapolate to the region  $0.4 < x_\gamma$ . A third fit was done in which the observed photon spectrum was freely fit to an exponential background plus a direct-photon signal model (Field or GS), rather than normalizing over a pre-specified  $x$ -interval. Figure 11 shows that this procedure satisfactorily reproduces continuum data below the  $\Upsilon(4S)$  resonance, verifying that it can be used to generate a rough estimate of the

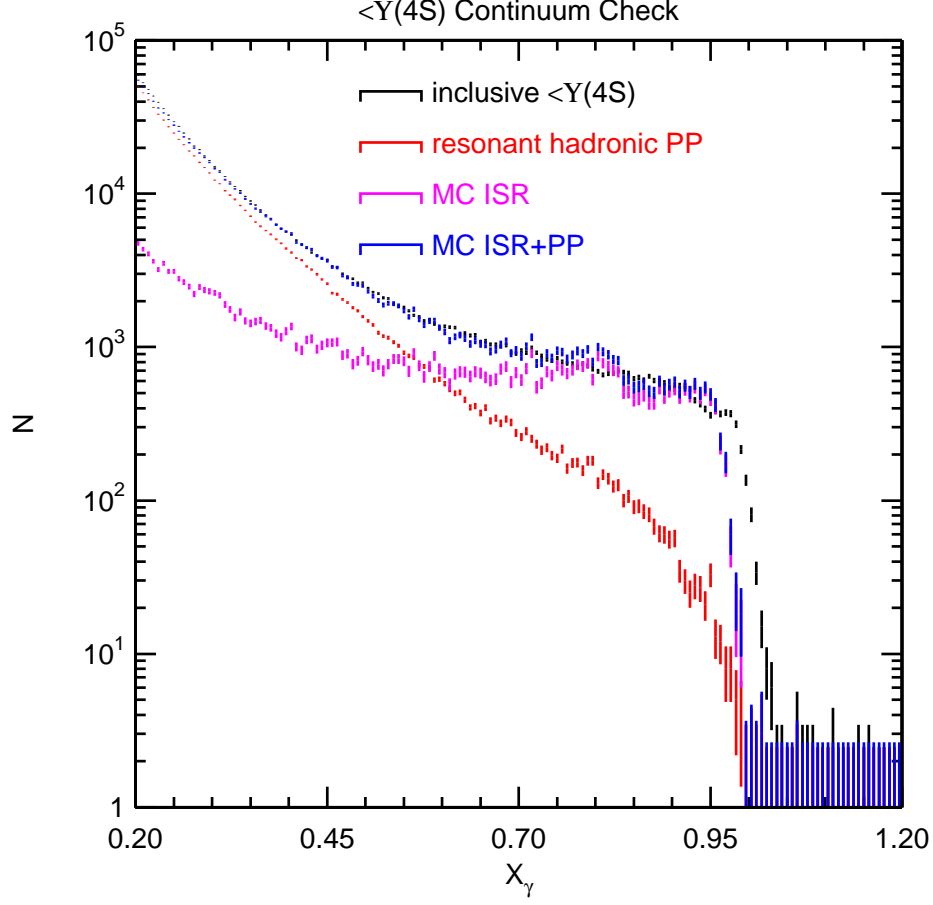


FIG. 6: Comparison of scaled  $x_\gamma$  spectra with two estimates of photon background, obtained using below- $\Upsilon(4S)$  data.

backgrounds.

### Model Fits

We estimate  $R_\gamma$  by extrapolating the observed photon spectrum down to  $x_\gamma=0$ . Since we have finite resolution, and since the photon-finding efficiency is momentum-dependent, two procedures may be used to compare with models. Either a migration-matrix can be determined from Monte Carlo simulations to estimate the bin-to-bin smearing, with a matrix-unfolding technique used to then compare with prediction, or the model can be first efficiency-attenuated (as a function of momentum), then smeared by the experimental resolution, to compare with the data. We have followed the latter procedure, floating only

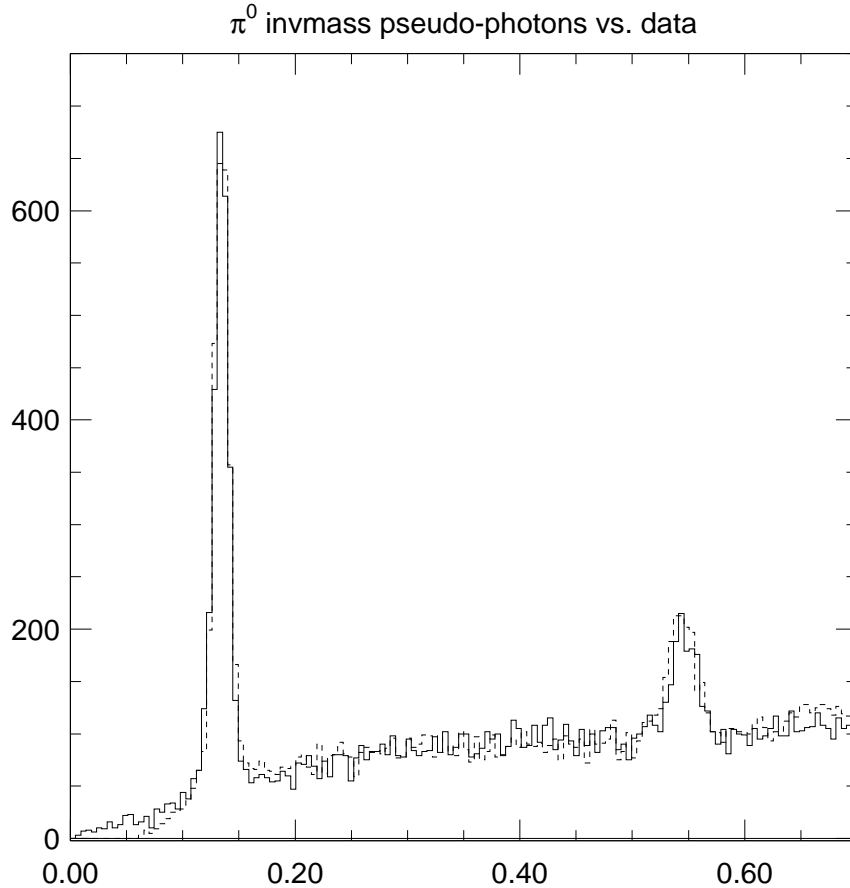


FIG. 7: The  $\pi^0$  and  $\eta$  yields between data (dashed) and pseudo-photon simulation (solid). The yields agree on the 2%-3% level. Discrepancy for  $m_{\gamma\gamma} < 50$  MeV is due to photon overlap effects in data under-corrected for in pseudo-photon simulation.

the normalization of the efficiency-attenuated, resolution-smearing model, in this analysis. Thus, to determine the percentage of direct photons within our fiducial acceptance, we used a Monte Carlo simulation of the direct photon events, incorporating measured photon-finding efficiencies and the QCD predictions of Koller and Walsh for the photon and gluon energy and angular distributions[5].

Figures 12, 13, and 14 show the fits to the Garcia-Soto model. We note, in some cases, an excess of photons in data as  $x_\gamma \rightarrow 1$ . Further examination of these events indicate that

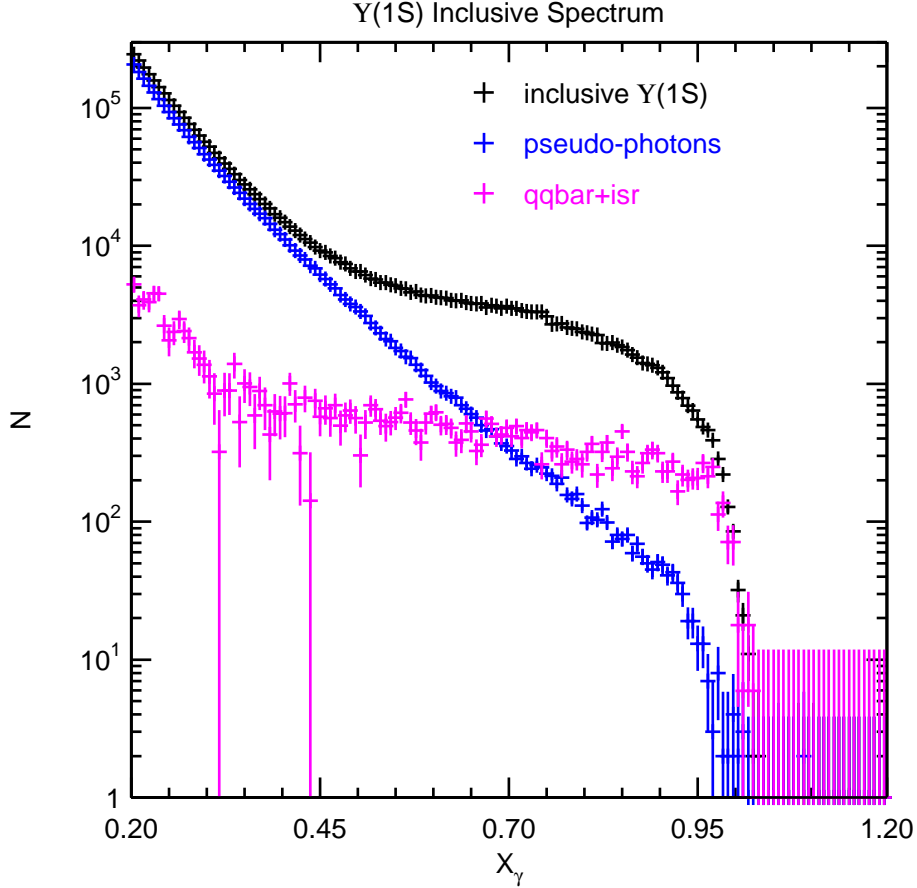


FIG. 8: Raw  $\Upsilon(1S)$  photon spectrum, with continuum contribution, and resonant non-direct pseudo-photons resulting from hadron decays overlaid.

these events are dominated by:  $e^+e^- \rightarrow \gamma\pi^+\pi^-\pi^+\pi^-$  (resonance structure of these 4-pion events has not yet been fully investigated).

Figures 15, 16, and 17 show fits obtained using a simple exponential parametrization of the background, with no pseudo-photon generation.

$$\Upsilon(2S) \rightarrow \pi^+\pi^-\Upsilon(1S); \Upsilon(1S) \rightarrow \gamma gg$$

Our large sample of  $\Upsilon(2S)$  decays, and the substantial  $\Upsilon(2S) \rightarrow \pi^+\pi^-\Upsilon(1S)$  branching fraction ( $\sim 0.19$ ) afford an opportunity to measure a ‘tagged’  $\Upsilon(1S)$  direct photon spectrum which circumvents all continuum backgrounds. In a given event taken at the  $\Upsilon(2S)$  center-of-mass energy, we calculate the mass recoiling against all oppositely-signed charged pion pairs (Figure 18). In each bin of recoil mass, we plot the spectrum of all high-energy photons in that event. A sideband subtraction around the  $\Upsilon(2S) \rightarrow \pi^+\pi^-\Upsilon(1S)$  recoil mass signal, at  $m_{recoil} \sim \Upsilon(1S)$  results in a tagged  $\Upsilon(1S)$  direct photon spectrum. Spectral shape and

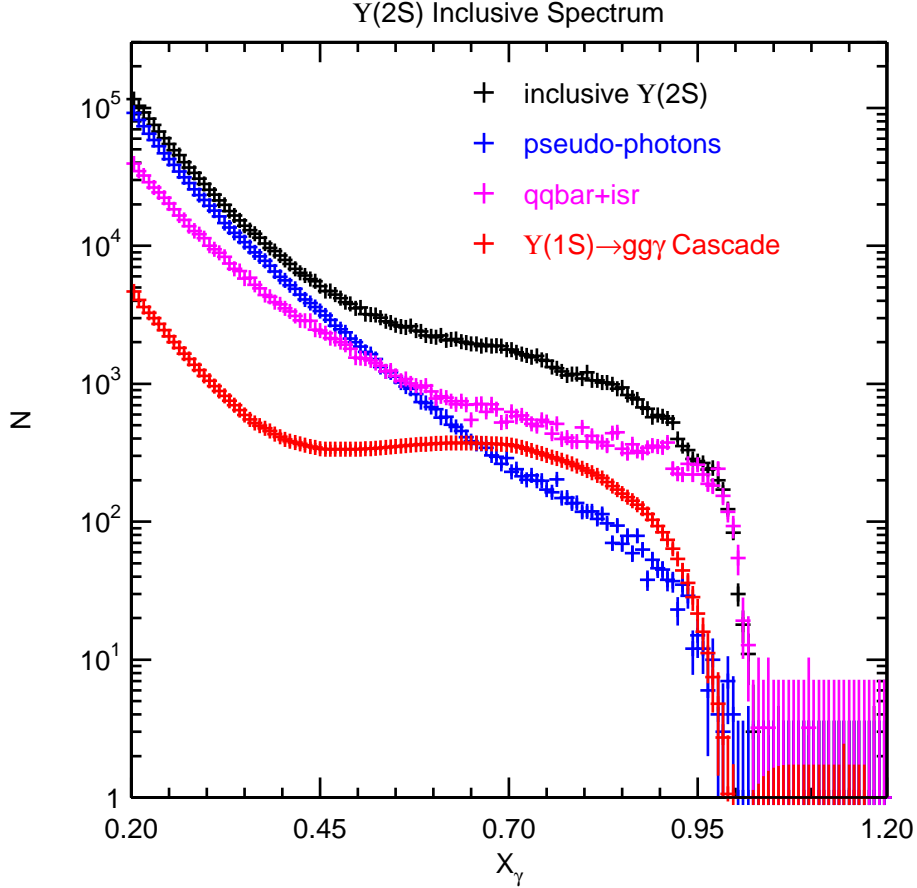


FIG. 9: Raw  $\Upsilon(2S)$  photon spectrum, with continuum contribution, resonant non-direct pseudo-photons, and the cascade contribution from  $\Upsilon(1S)$  decays overlaid.

$R_\gamma$  values obtained this way are consistent with our other estimates.

### Determination of $N_{ggg}$

To determine the number of three gluon events  $N_{ggg}$  from the number of observed  $\Upsilon(1S)$  hadronic events  $N_{had}^{\Upsilon(1S)}$ , we first subtracted the number of  $\Upsilon(1S)$  continuum events  $N_{cont}^{\Upsilon(1S)}$  from the observed number of below  $\Upsilon(1S)$  continuum events  $N_{cont}^{ECM=9.43 \text{ GeV}}$ :

$$N_{cont}^{\Upsilon(1S)} = N_{cont}^{ECM=9.43 \text{ GeV}} \cdot \frac{\mathcal{L}_{\Upsilon(1S)} s_{cont}}{\mathcal{L}_{cont} s_{1S}}. \quad (4)$$

where the factor  $\frac{\mathcal{L}_{\Upsilon(1S)}}{\mathcal{L}_{cont}}$  arises from the number of events  $N = \mathcal{L} \cdot \sigma$ , and  $s \equiv ECM^2$ . From the observed number of resonant hadronic events  $N_{had}^{\Upsilon(1S)}$ , and knowing the branching fractions and efficiencies for  $\Upsilon(1S) \rightarrow q\bar{q}$ ,  $\Upsilon(1S) \rightarrow gg\gamma$ , and  $\Upsilon(1S) \rightarrow ggg$  the number of  $\Upsilon(1S) \rightarrow ggg$  events can be inferred. For  $\Upsilon(1S) \rightarrow q\bar{q}$ , e.g., we use the  $\Upsilon(1S) \rightarrow \mu^+\mu^-$  branching fraction



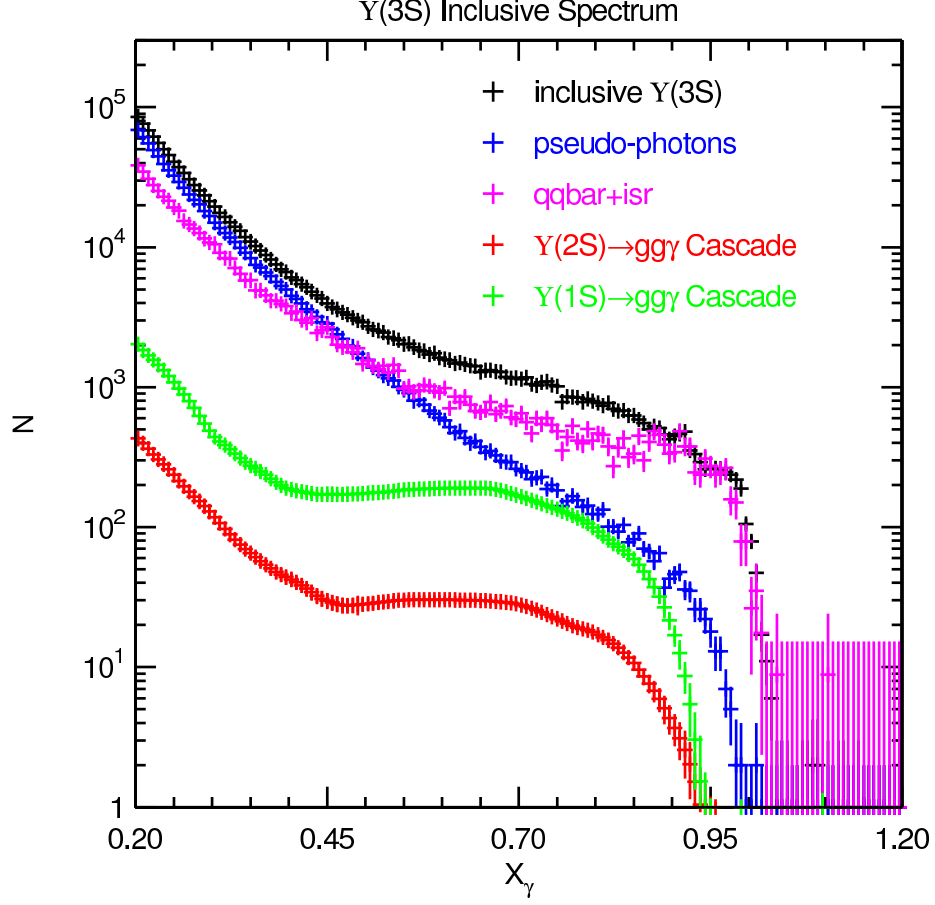


FIG. 10: Raw  $\Upsilon(3S)$  photon spectrum, with continuum contribution, resonant non-direct pseudo-photons resulting from hadron decays, and the cascade contribution from  $\Upsilon(2S)$  and  $\Upsilon(1S)$  decays overlaid.

$B_{\mu\mu} = 0.0248$  [22, 23], and  $R_{\Upsilon(1S)} = \sigma(e^+e^- \rightarrow \Upsilon(1S) \rightarrow q\bar{q})/\sigma(e^+e^- \rightarrow \Upsilon(1S) \rightarrow \mu^+\mu^-) = 3.51$  [24, 25]:

$$N_{q\bar{q}} = R_{\Upsilon(1S)} \cdot B_{\mu\mu} \epsilon_{q\bar{q}} \cdot \frac{N_{had}^{\Upsilon(1S)}}{(1 - 3B_{\mu\mu})\bar{\epsilon}_{had}} \quad (5)$$

with  $\bar{\epsilon}_{had}$  the average hadronic event reconstruction efficiency. Using  $\mathcal{B}(\Upsilon(2S) \rightarrow \Upsilon(1S)X) = (32 \pm 2)\%$ ,  $\mathcal{B}(\Upsilon(3S) \rightarrow \Upsilon(2S)X) = (10.6 \pm 0.8)\%$ , and  $\mathcal{B}(\Upsilon(3S) \rightarrow \Upsilon(1S)X) = (12 \pm 1)\%$ , a three-gluon decay fraction for the three resonances  $f_{ggg} = 82 \pm 2\%$ ,  $40 \pm 4\%$ , and  $41 \pm 2\%$ , respectively, as well as continuum-subtracted, efficiency-corrected hadronic event yields  $N_{had}(1S) = 19791348 \pm 56555 \pm 656528$ ,  $N_{had}(2S) = 8009386 \pm 58154 \pm 208873$ , and  $N_{had}(3S) = 4653678 \pm 10215 \pm 23372$ , we obtained a value for  $R_\gamma$  for each of the resonances. More details on this subtraction are

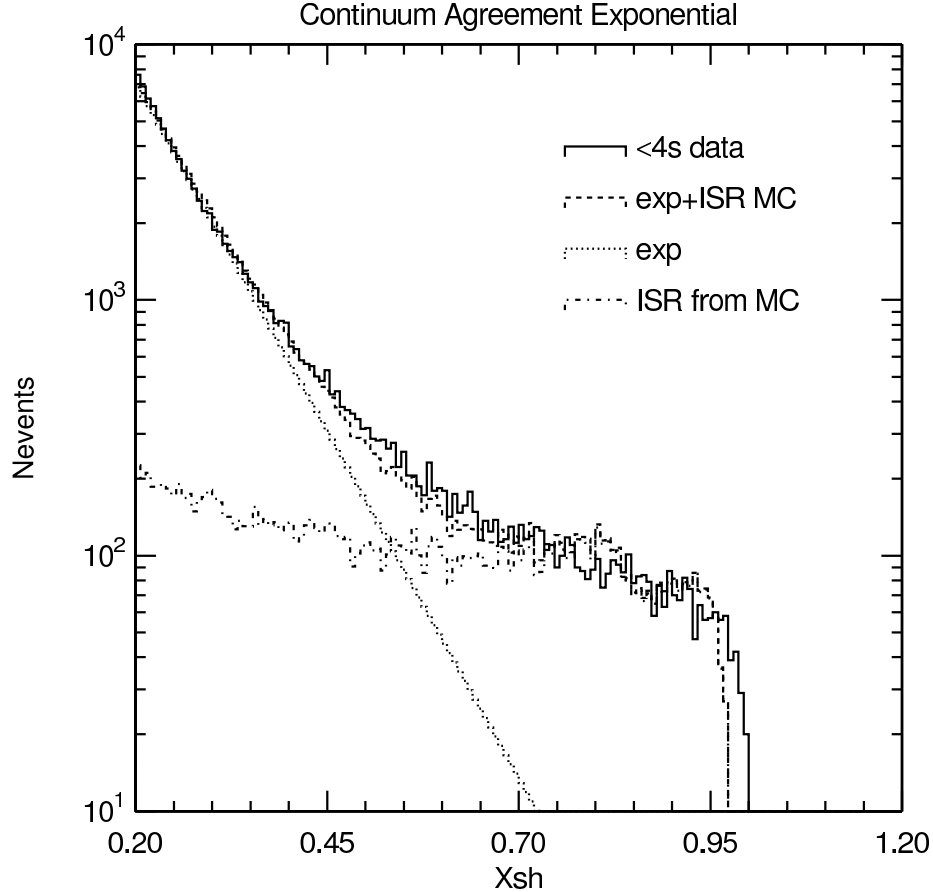


FIG. 11: Subtraction of backgrounds using an exponential (below-4S continuum data), with floating normalization to estimate the non-direct photon spectrum. The exponential, plus initial state radiation, gives a fair match to the observed spectrum, although the background is clearly underestimated in the intermediate region of the momentum spectrum.

presented in Table II and also in the accompanying appendix.

Table III presents our numerical results for the extracted branching fractions.

### Systematic errors

We identify and estimate systematic errors as follows:

1. For the  $\Upsilon(1S)$ , the uncertainty in  $N_{ggg}$  is based on the CLEO estimated three-gluon event-finding efficiency. For the  $\Upsilon(2S)$  and  $\Upsilon(3S)$  decays, the uncertainty in  $N_{ggg}$  folds in uncertainties in the tabulated radiative and hadronic transition decay rates from

Event Type	$\epsilon$
$\Upsilon(1S) \rightarrow ggg$	$0.953 \pm 0.003$
$\Upsilon(1S) \rightarrow gg\gamma$	$0.751 \pm 0.007$
$\Upsilon(1S) \rightarrow q\bar{q}$	$0.871 \pm 0.005$
$\Upsilon(2S) \rightarrow ggg$	$0.956 \pm 0.003$
$\Upsilon(2S) \rightarrow gg\gamma$	$0.776 \pm 0.007$
$\Upsilon(2S) \rightarrow q\bar{q}$	$0.882 \pm 0.005$
$\Upsilon(2S) \rightarrow \Upsilon(1S) + X \rightarrow ggg$	$0.956 \pm 0.003$
$\Upsilon(2S) \rightarrow \Upsilon(1S) + X \rightarrow gg\gamma$	$0.778 \pm 0.007$
$\Upsilon(2S) \rightarrow \Upsilon(1S) + X \rightarrow q\bar{q}$	$0.891 \pm 0.005$
$\Upsilon(2S) \rightarrow \chi_{bn}(1P) \rightarrow gg (n = 0, 1, 2)$	$0.933 \pm 0.004$
$\Upsilon(3S) \rightarrow ggg$	$0.955 \pm 0.003$
$\Upsilon(3S) \rightarrow gg\gamma$	$0.765 \pm 0.007$
$\Upsilon(3S) \rightarrow q\bar{q}$	$0.881 \pm 0.005$
$\Upsilon(3S) \rightarrow \Upsilon(2S) + X \rightarrow ggg$	$0.958 \pm 0.003$
$\Upsilon(3S) \rightarrow \Upsilon(2S) + X \rightarrow gg\gamma$	$0.765 \pm 0.007$
$\Upsilon(3S) \rightarrow \Upsilon(2S) + X \rightarrow q\bar{q}$	$0.877 \pm 0.005$
$\Upsilon(3S) \rightarrow \Upsilon(1S) + X \rightarrow ggg$	$0.961 \pm 0.003$
$\Upsilon(3S) \rightarrow \Upsilon(1S) + X \rightarrow gg\gamma$	$0.789 \pm 0.006$
$\Upsilon(3S) \rightarrow \Upsilon(1S) + X \rightarrow q\bar{q}$	$0.90 \pm 0.07$
$\Upsilon(3S) \rightarrow \chi_{bn}(1P) \rightarrow gg (n = 0, 1, 2)$	$0.819 \pm 0.006$
$\Upsilon(3S) \rightarrow \chi_{bn}(2P) \rightarrow gg (n = 0, 1, 2)$	$0.929 \pm 0.004$
$\Upsilon$ Resonance	$N_{total}(\Upsilon(nS)) (10^6)$
$\Upsilon(1S)$	$21.4 \pm 0.7$
$\Upsilon(2S)$	$8.5 \pm 0.2$
$\Upsilon(3S)$	$5.01 \pm 0.03$
Fraction	$f$
$f(\Upsilon(1S) \rightarrow ggg)$	$0.82 \pm 0.02$
$f(\Upsilon(2S) \rightarrow ggg)$	$0.40 \pm 0.04$
$f(\Upsilon(3S) \rightarrow ggg)$	$0.41 \pm 0.02$
$f(\Upsilon(2S) \rightarrow \Upsilon(1S) + X)$	$0.32 \pm 0.02$
$f(\Upsilon(3S) \rightarrow \Upsilon(2S) + X)$	$0.11 \pm 0.01$
$f(\Upsilon(3S) \rightarrow \Upsilon(1S) + X)$	$0.12 \pm 0.01$

TABLE II: Efficiencies for the reconstruction in MC of the various types of events considered in this analysis, the total number of  $\Upsilon(1S)$ ,  $\Upsilon(2S)$  and  $\Upsilon(3S)$  events calculated from these efficiencies using the procedure outlined in the appendix of this paper, and the fractions of these totals which were used to obtain the  $\Upsilon \rightarrow ggg$  denominator in our measurements of  $R_\gamma$ , and to scale the direct photon cascade spectra in our  $\Upsilon(2S)$  and  $\Upsilon(3S)$  subtractions. These fractions were obtained from the PDG [22] and include recent CLEO  $\chi_b$  measurements. The presented errors on the efficiencies are statistical only.

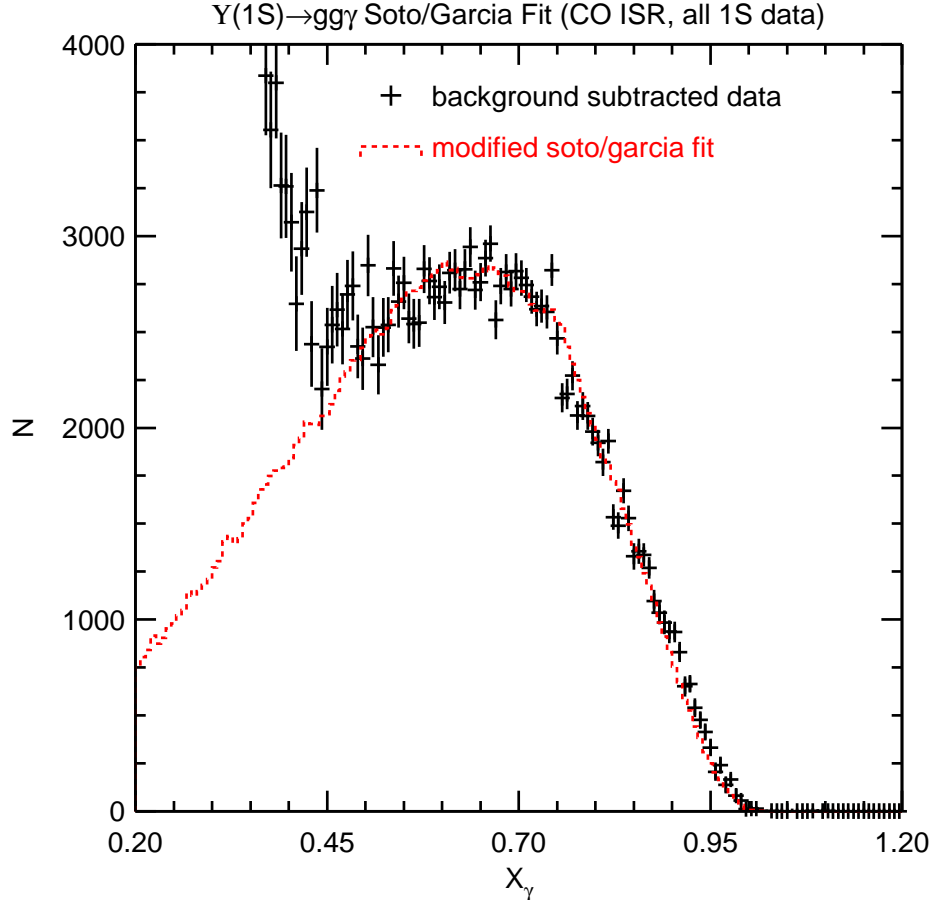


FIG. 12: Fit to background subtracted data ( $\Upsilon(1S)$  data), using explicit continuum data subtraction. Direct spectrum fit using Garcia-Soto model.

the parent resonances, which are necessary for determining  $N_{gg\gamma}$  as well as the magnitude of the cascade subtractions. The cascade subtraction errors include statistical uncertainties in the branching fractions of Upsilon resonances into final states other than 3-gluon and  $gg\gamma$ ; these errors are assessed by shifting all relevant decay branching fractions by  $\pm 1\sigma$ .

2. Background normalization and background shape uncertainty are evaluated redundantly as follows:

We determine the branching fractions with and without an explicit  $\pi^0$  veto on the background.

We measure the internal consistency of our results using different sub-samples of our  $\Upsilon(1S)$ , (2S) and (3S) samples.

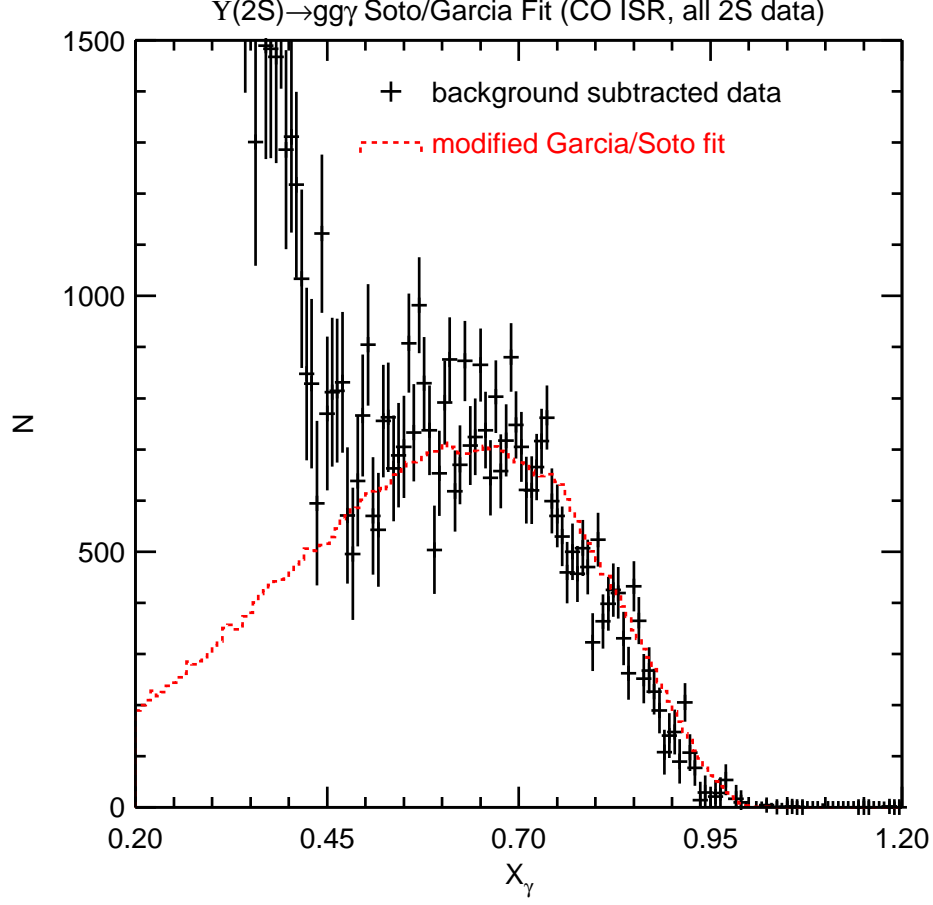


FIG. 13: Fit to background subtracted data ( $\Upsilon(2S)$  data), using explicit continuum data subtraction and explicit subtraction of  $\Upsilon(1S)$  cascade contributions. Direct spectrum fit using Garcia-Soto model.

Bias in background subtraction can also be estimated using Monte Carlo simulations. We treat the simulation as we do data, and generate pseudo-photons based on the Monte Carlo identified charged pion tracks. After subtracting the pseudo-photon spectrum from the full Monte Carlo photon spectrum, we can compare our pseudo-photon and ISR-subtracted spectrum with the known spectrum that was generated as input to the Monte Carlo detector simulation. For the  $\Upsilon(1S)$ ,  $\Upsilon(2S)$ , and  $\Upsilon(3S)$ , we observe fractional deviations of  $-6.6\%$ ,  $-5.7\%$ , and  $+6.1\%$  between the input spectrum and the pseudo-photon background-subtracted spectrum. To the extent that the initial state radiation estimate and the photon-finding efficiency are obtained from the same Monte Carlo simulations, this procedure is mainly a check of our generation of the pseudo-photon background and the correlation of  $\pi^0$  decay angle with efficiency.

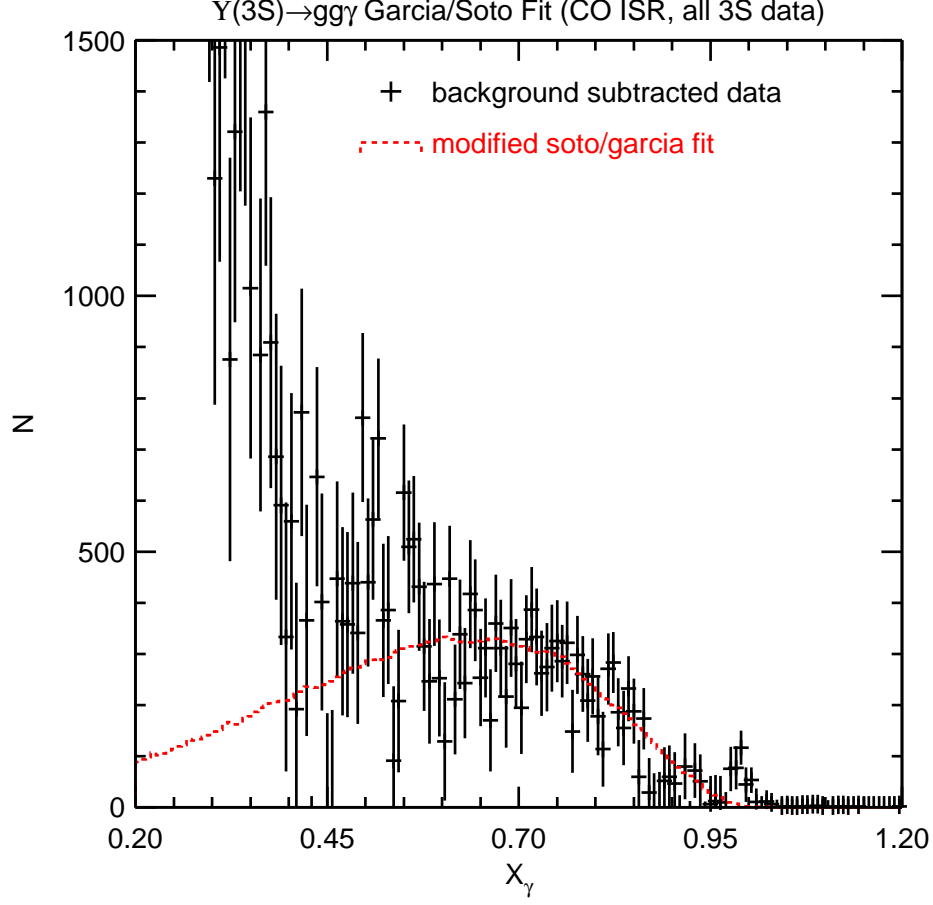


FIG. 14: Fit to background subtracted data ( $\Upsilon(3S)$  data), using explicit continuum data subtraction and explicit subtraction of  $\Upsilon(1S)$  and  $\Upsilon(2S)$  cascade contributions. Direct spectrum fit using Garcia-Soto model.

We extract the direct photon branching fractions using a flat  $\pi^0 : \pi^+$  isospin ratio of 0.5, compared to the  $\pi^0 : \pi^+$  ratio based on Monte Carlo simulations, including all our event selection and charged tracking and charged particle identification systematics ( $\sim 0.53$ , Figure 2)

We compare the branching fractions based on a direct continuum data subtraction (including ISR) vs. a Monte Carlo simulated ISR spectrum subtraction, which relies on the pseudo-photon generator to simulate the contribution from continuum decays of  $\pi^0$ ,  $\eta$ ,  $\eta'$  and  $\omega$ . These are additionally compared with the  $R_\gamma$  values obtained using an exponential parametrization of the background.

Our uncertainty in the magnitude of the continuum subtraction is due to our uncertainty in the on-resonance vs. off-resonance luminosity scaling ( $< 1\%$ , absolute).

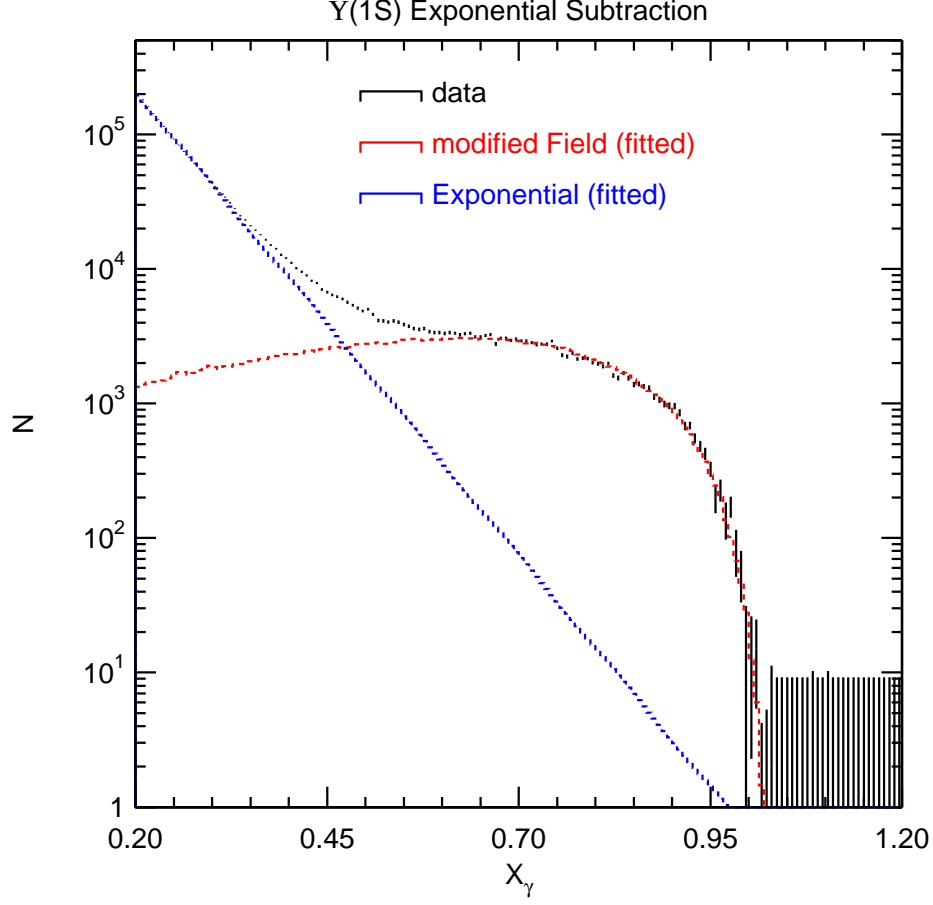


FIG. 15: Subtraction of backgrounds using an exponential ( $\Upsilon(1S)$  data), with floating normalization to estimate the non-direct photon spectrum. Direct spectrum fit using Field.

3. Model dependence of the extracted total decay rate is estimated by: i) determining the consistency of our data to a given model (either Field or Garcia-Soto) by fitting our data in two distinct photon momentum intervals ( $0.45 \leq x_\gamma \leq 0.65$  vs.  $0.65 \leq x_\gamma \leq 0.95$ ), and also by ii) comparing the results obtained from fits to the Field model with results obtained from the fits to the Garcia-Soto model over the full fitted  $x_\gamma$  interval. (We currently assume the Koller-Walsh prescription for the angular distribution is correct, and assign no systematic error for a possible corresponding uncertainty.) The irreducible model-dependence error is presented as the last error in our quoted branching fraction.

Note that variation of the fit region also probes the uncertainty due to event selection requirements. Most important is the minimum charged track multiplicity requirement, which is increasingly significant as  $x_\gamma \rightarrow 1$  and the available phase space for hadroniza-

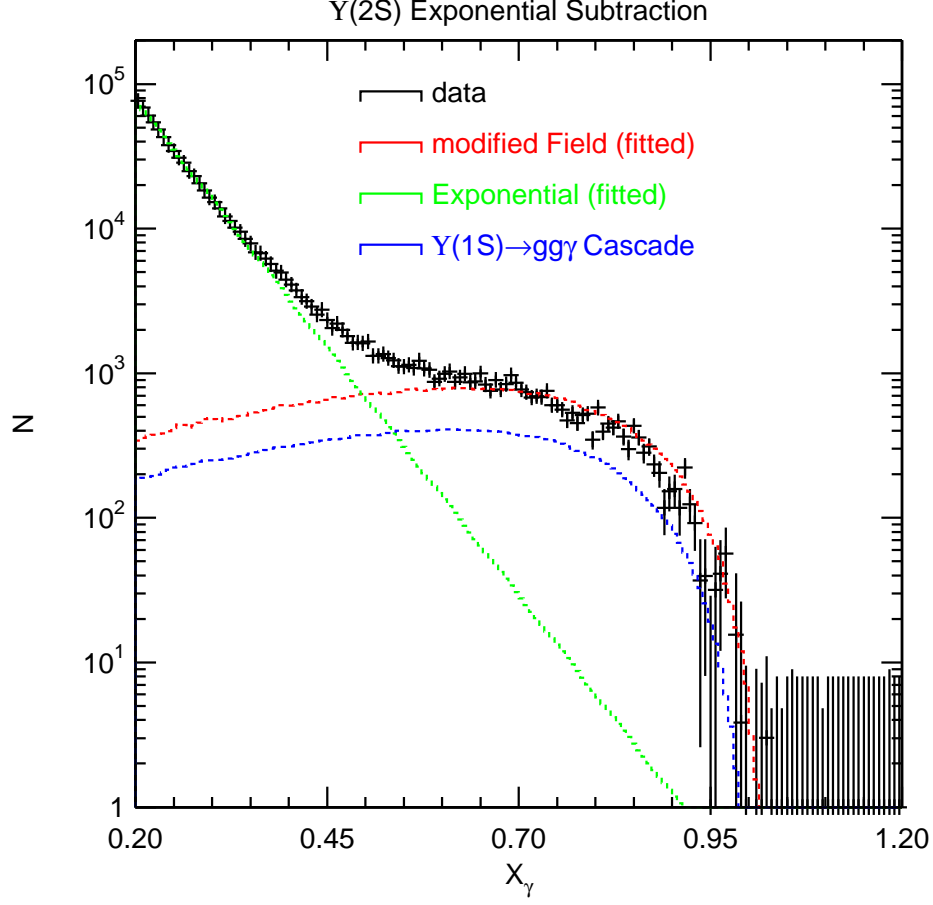


FIG. 16: Subtraction of backgrounds using an exponential ( $\Upsilon(2S)$  data), with floating normalization to estimate the non-direct photon spectrum. Direct spectrum fit using Field.

tion of the recoil gluons becomes vanishingly small. By contrast, the lower- $x_\gamma$  region is substantially less sensitive to such phase space effects. The consistency of the tagged  $\Upsilon(1S)$  analysis (sensitive to  $\Upsilon(1S)$  charged multiplicities  $\geq 2$ ) and the direct analysis also limits the magnitude of this systematic error.

Table IV summarizes the potential systematic errors studied in this analysis and their estimated effect on  $R_\gamma$ .

### Comparison with previous analyses

Table V compares the results of this analysis with those obtained by previous experiments in which the observed number of  $\Upsilon(1S) \rightarrow gg\gamma$  events were determined using Field's



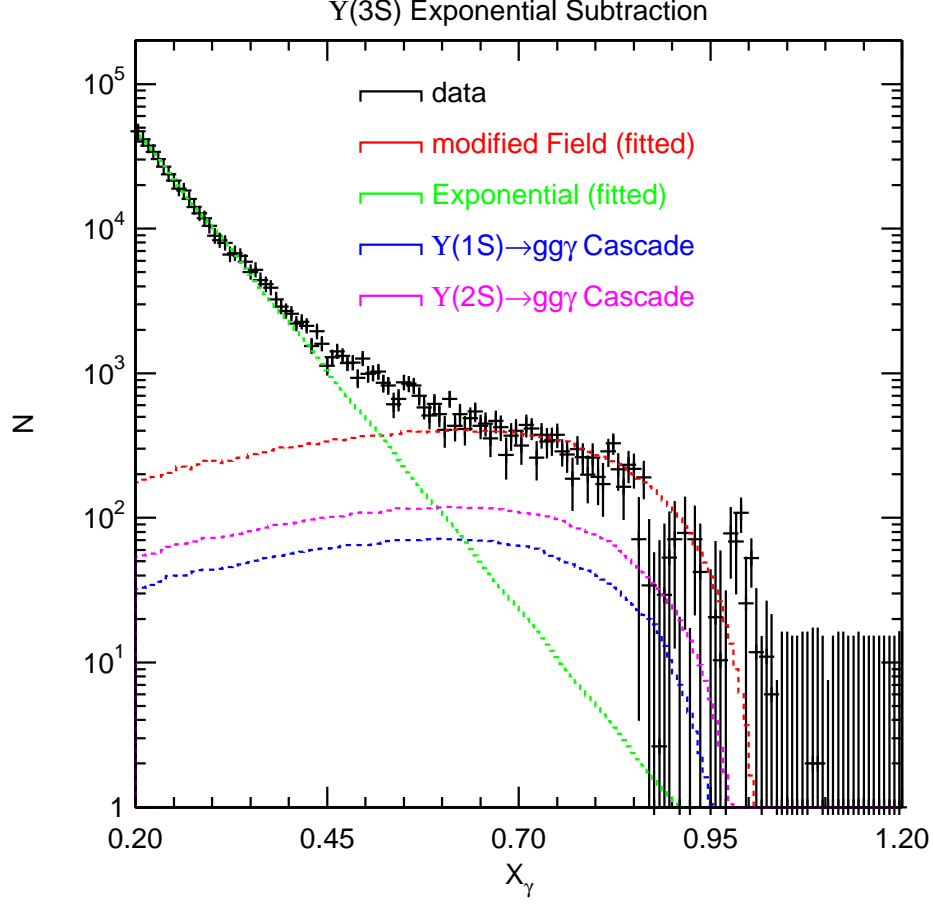


FIG. 17: Subtraction of backgrounds using an exponential ( $\Upsilon(3S)$  data), with floating normalization to estimate the non-direct photon spectrum. Direct spectrum fit using Field.

theoretical model only.

### Summary

We have re-measured the  $\Upsilon(1S) \rightarrow \gamma gg / \Upsilon(1S) \rightarrow ggg$  branching fraction ( $R_\gamma$ ), obtaining agreement with previous results. We also have made first measurements of  $R_\gamma(2S)$  and  $R_\gamma(3S)$ . Our results are, within errors, consistent with the naive expectation that  $R_\gamma(1S) \sim R_\gamma(2S) \sim R_\gamma(3S)$ , although that equality does not hold for the recent CLEO measurements of  $B_{\mu\mu}$  for the three resonances[4]. Assuming an energy scale equal to the parent  $\Upsilon$  resonance, our values of  $R_\gamma$  for  $\Upsilon(1S) \rightarrow gg\gamma$ ,  $\Upsilon(2S) \rightarrow gg\gamma$  and  $\Upsilon(3S) \rightarrow gg\gamma$  imply values of the strong coupling constant ( $0.1093 \pm 0.0001 \pm 0.0048 \pm 0.0029$ ,  $0.0978 \pm 0.0005 \pm 0.0089 \pm 0.0029$  and

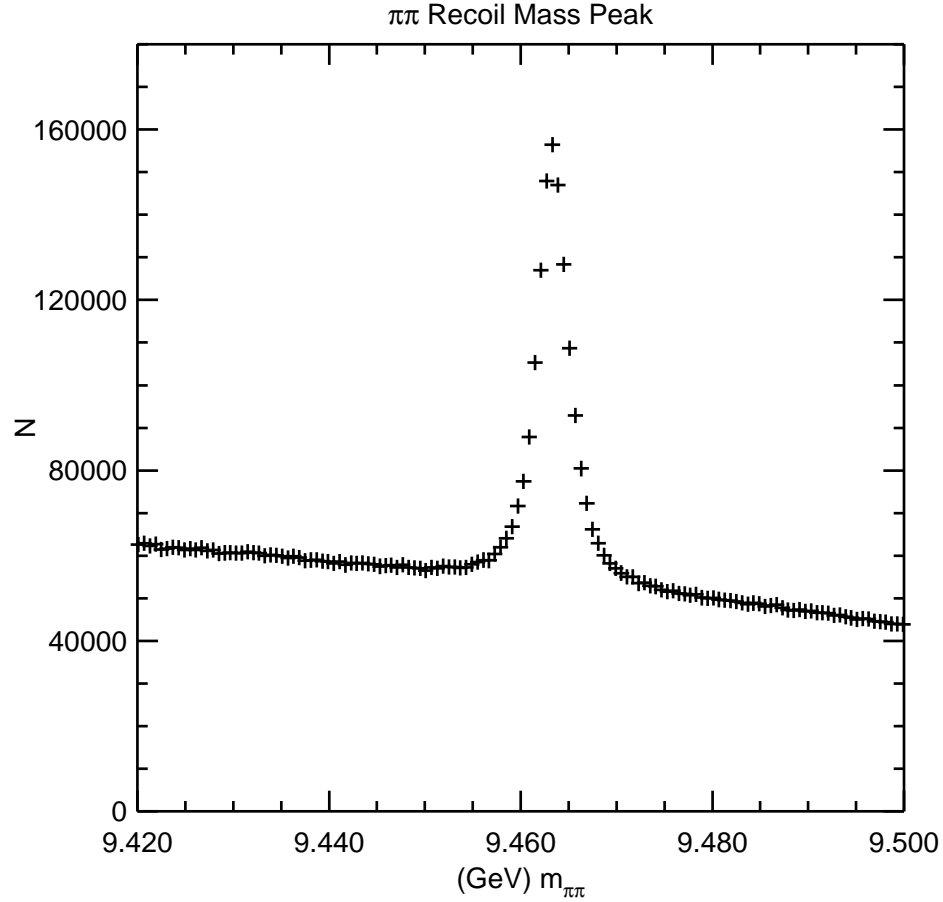


FIG. 18: Mass recoiling against oppositely signed charged pion pairs,  $\Upsilon(2S)$  data.

$0.1088 \pm 0.0006 \pm 0.0075 \pm 0.0006$ , respectively) which are consistent with measurements made at the Z-pole (Appendix II).

### Acknowledgments

We thank Adam Liebovich, Sean Fleming, Xavier Garcia and Joan Soto for useful discussions. We gratefully acknowledge the effort of the CESR staff in providing us with excellent luminosity and running conditions. This work was supported by the National Science Foun-

$X \rightarrow gg\gamma; X=$	Background	Field $R_\gamma$	GS $R_\gamma$
$\Upsilon(1S)$	Exponential	$(3.0 \pm 0.3)\%$	$(2.7 \pm 0.3)\%$
$\Upsilon(1S)$	PP (MC ISR)	$(2.89 \pm 0.01)\%$	$(2.61 \pm 0.01)\%$
$\Upsilon(1S)$	PP (CO ISR)	$(3.05 \pm 0.02)\%$	$(2.76 \pm 0.01)\%$
$\Upsilon(1S) (\Upsilon(2S) \rightarrow \pi\pi\Upsilon(1S)\text{-tagged})$	PP (no ISR)	$(2.88 \pm 0.06)\%$	$(2.60 \pm 0.06)\%$
$\Upsilon(2S)$	Exponential	$(4.0 \pm 0.5)\%$	$(3.7 \pm 0.3)\%$
$\Upsilon(2S)$	PP (MC ISR)	$(3.54 \pm 0.05)\%$	$(3.20 \pm 0.05)\%$
$\Upsilon(2S)$	PP (CO ISR)	$(3.78 \pm 0.06)\%$	$(3.41 \pm 0.05)\%$
$\Upsilon(3S)$	Exponential	$(3.5 \pm 0.1)\%$	$(3.35 \pm 0.09)\%$
$\Upsilon(3S)$	PP (MC ISR)	$(2.76 \pm 0.07)\%$	$(2.49 \pm 0.06)\%$
$\Upsilon(3S)$	PP (CO ISR)	$(2.9 \pm 0.1)\%$	$(2.6 \pm 0.1)\%$

TABLE III: Summary of Measurements. “PP” denotes Pseudo-Photon background, “MC ISR” implies that Monte Carlo simulations of initial state radiation were used to subtract the ISR background. “CO ISR” implies that data ISR was subtracted directly using below-resonance data. Values obtained using an exponential parametrization have had systematic errors (reflecting sensitivity to region chosen for scale normalization of exponential outside the peak region; for this estimate, branching fractions were compared using the regions  $0.2 < x_\gamma < 0.3$  or  $0.3 < x_\gamma < 0.4$  to set the scale of the exponential and extrapolate under the signal in the higher-x region) added in quadrature with the statistical error. Note that  $\Upsilon(2S)$   $R_\gamma$  values have been corrected for  $\Upsilon(1S) \rightarrow gg\gamma$  contamination;  $\Upsilon(3S)$   $R_\gamma$  values have been corrected for both  $\Upsilon(2S) \rightarrow gg\gamma$ , and also  $\Upsilon(1S) \rightarrow gg\gamma$  contamination.

dation and the U.S. Department of Energy.

- 
- [1] S. J. Brodsky, G. P. Lepage and P. B. Mackenzie, Phys. Rev. **D 28**, 228 (1983).
  - [2] S.J. Brodsky, T.A.DeGrand, R.R. Horgan and D.G. Coyne, Phys. Lett. **B73**, 203 (1978); K. Koller, and T. Walsh, Nucl. Phys. **B140**, 449 (1978).
  - [3] S.A. Larin, T. van Ritbergen, and J.A.M. Vermaseren, Phys. Lett. **B400**, 379 (1997).
  - [4] G.S. Adams et al., CLEO Collab., Phys. Rev. Lett. **94**, 012001 (2005).
  - [5] K. Koller, and T. Walsh, ref [2].
  - [6] R.D. Field, Phys. Lett. **B133**, 248 (1983).
  - [7] R.D. Schamberger et al., CUSB Collab. Phys. Lett. **B138**, 225 (1984).
  - [8] S.E. Csorna et al., CLEO Collab., Phys. Rev. Lett. **56**, 1222 (1986).
  - [9] D.M. Photiadis, Phys. Lett. **B164**, 160 (1985).
  - [10] A. Bizzeti et al., CRYSTAL BALL Collab., Phys. Lett. **B267**, 286 (1991).
  - [11] H. Albrecht et al., ARGUS Collab., Phys. Lett. **B199**, 291 (1987).
  - [12] S. Catani and F. Hautmann, Nucl. Phys. **B**, Proc. Suppl. **39BC**, 359 (1995).
  - [13] M. Yusuf and P. Hoodbhoy, Phys.Rev. **D54**, 3345 (1996).
  - [14] S. Fleming and A. Leibovich, Phys. Rev. **D67**, 074035 (2003); S. Fleming and A. Leibovich, Phys. Rev. Lett. **90**, 032001 (2003).
  - [15] S. Fleming and A. Leibovich, Phys. Rev. **D68** 094011, (2003).
  - [16] X. Garcia and J. Soto, Phys. Rev. **D69**, 114006 (2004).
  - [17] CLEO Collab., Y. Kubota et al., Nucl. Inst. Meth. **A 320**, 66 (1992).

Source	$\delta R_\gamma(1S/2S/3S)(\%)$
Diff(MC Glevel, MC analyzed)	0.18/0.19/0.20
Background Shape/Norm, including:	
With/Without a $\pi^0$ veto	0.07/0.07/0.07
MC vs. CO subtraction	<0.08/0.11/0.08
Isospin Assumption	0.01/0.01/0.01
$\epsilon_{ggg}$	0.11/0.34/0.12
Cascade subtraction	0/0.15/0.01
Luminosity and S scaling	0.01/0.01/0.01
Fit interval sensitivity (0.45→0.65 v. 0.65→0.95)	0.002/0.36/0.27
Model Dependence (GS vs. Field)	0.14/0.18/0.03
Consistency of different datasets	0.01/0.09/0.09
<b>Total Systematic Error</b>	<b>0.24/0.58/0.38</b>

TABLE IV: Current Systematic Errors. The uncertainty in the multiplicity modelling is smaller for the  $\Upsilon(1S)$  based on the observed consistency of the tagged  $\Upsilon(2S) \rightarrow \Upsilon(1S)\pi^+\pi^-$  (sensitive to lower multiplicities than for the direct analysis).

Experiment	$R_\gamma(\%)$
CLEO 1.5 [8]	$2.54 \pm 0.18 \pm 0.14$
ARGUS [11]	$3.00 \pm 0.13 \pm 0.18$
XBAL [10]	$2.7 \pm 0.2 \pm 0.4$
CLEO II [20]	$2.77 \pm 0.04 \pm 0.15$
This measurement	$2.80 \pm 0.007 \pm 0.24 \pm 0.14$
$\Upsilon(2S)$	$3.45 \pm 0.03 \pm 0.58 \pm 0.18$
$\Upsilon(3S)$	$2.89 \pm 0.03 \pm 0.38 \pm 0.03$

TABLE V: Comparison with other experiments. Errors are statistical, systematic, and model (Field vs. Garcia/Soto), respectively.

- [18] D. Peterson *et al.*, Nucl. Inst. Meth. **A 478**, 142 (2002).
- [19] M. Artuso *et al.*, Nucl. Inst. Meth. **A 502**, 91 (2003).
- [20] B. Nematy *et al.* CLEO Collab., Phys. Rev. **D55**, (1997).
- [21] .T. M. Yan, Phys. Rev. **D 22**, 1652 (1980).
- [22] Review of Particle Properties, Particle Data Group, <http://pdg.lbl.gov>.
- [23] S. B. Athar *et al.*, CLEO Collab., Phys. Rev. Lett. **94**, 012001 (2005).
- [24] H. Albrecht *et al.*, ARGUS Collab., Z. Phys. **C54**, 13 (1992).
- [25] R. Ammar *et al.*, Phys. Rev. **D57**, 1350 (1998)
- [26] P. B. Mackenzie and G. Peter Lepage, in *Perturbative Quantum Chromodynamics*, Conf. Proceed., Tallahassee, AIP, New York, (1981).
- [27] W. A. Bardeen *et al.*, Phys. Rev. **D 18**, 3998 (1978).
- [28] P. B. Mackenzie and G. Peter Lepage, Phys. Rev. Lett. **47**, 1244 (1981).
- [29] G. Grunberg, Phys. Lett. **B 95**, 70 (1980).
- [30] P.M. Stevenson, Phys. Rev. **D 23**, 2916 (1981).

- [31] S. Sanghera, Int'l Journal of Mod. Phys. **A 9**, 5473 (1994).  
[32] W. J. Marciano, Phys. Rev. **D 29**, 580 (1984).  
[33] A. C. Benvenuti, BCDMS Collab., Phys. Lett **B 223**, 490 (1989).

### Appendix I) Calculation of 3-gluon events and cascade corrections

The procedure for determining the denominator in the  $R_\gamma$  measurement can be summarized as follows: a) define hadronic event selection requirements, specifically excluding leptonic decays, b) perform a continuum subtraction to isolate resonant decays into hadrons, c) divide the observed number of resonant decays into hadrons by the average hadronic event-finding efficiency to determine the corrected number of true hadronic events d) correct by the fraction of “unseen” decays (leptonic modes) to determine the total number of resonant events, e) subtract off the number of non- $ggg$  decays using tabulated values, leaving  $N_{ggg}$  three-gluon events remaining.

Following this approach, we now outline the determination of the denominator ( $N_{ggg,1S}$ ), assuming that we measure a total number  $N_{had,total}^{obs}(ECM = 9.46)$  events passing hadronic event selection requirements at the  $\Upsilon(1S)$  resonance. In what follows,  $N_{had,CO}^{obs}$  is the number of events passing hadronic event selection requirements on the continuum 30 MeV below the peak,  $\epsilon_{ggg,1S}/\epsilon_{had,CO}$  is the efficiency for reconstructing either a hadronic  $\Upsilon(1S) \rightarrow ggg$  event or an  $e^+e^- \rightarrow q\bar{q}$  event on the continuum,  $N_{had,1S}$  designates the true number of total hadronic  $\Upsilon(1S)$  events,  $\mathcal{L}$  is the luminosity,  $B_{\mu\mu,1S}$  is the branching fraction for  $\Upsilon(1S) \rightarrow \mu\mu$ , and  $R = 3.51 \pm 0.05$  is the ratio of  $e^+e^- \rightarrow q\bar{q}/e^+e^- \rightarrow \mu^+\mu^-$  at our center-of-mass energy.

The total number of measured hadronic events, at the  $\Upsilon(1S)$  center-of-mass energy (ECM=9.46 GeV) is:

$$N_{had,total}^{obs}(ECM = 9.46) = N_{l+l^-,1S}\epsilon_{l^+,l^-,1S} + N_{ggg,1S}\epsilon_{ggg,1S} + N_{gg\gamma,1S}\epsilon_{gg\gamma,1S} + N_{q\bar{q},1S}\epsilon_{q\bar{q},1S} + N_{had,CO}(ECM = 9.46)\epsilon_{had,CO}(ECM = 9.46).$$

The minimum multiplicity requirement, ( $N_{charged} \geq 4$ ), as well as the explicit muon, electron, and 1 vs. 3 topology veto removes virtually all contributions from dilepton events and tau-pairs (3 vs. 3 tau pairs will still contribute, although such events correspond to less than 2% of all dileptonic decays of the  $\Upsilon(1S)$  resonance); this contribution is set to zero in what follows. Assuming that the backgrounds and efficiencies for continuum running at ECM=9.46 GeV are the same as at ECM=9.43 GeV, we subtract the continuum directly from  $N_{had,total}^{obs}(ECM = 9.46)$ :

$$N_{had,CO}(ECM = 9.46) = N_{had,CO}(ECM = 9.43) \times \frac{\mathcal{L}(ECM=9.46)}{\mathcal{L}(ECM=9.43)} \times \frac{9.43^2}{9.46^2},$$

leaving the observed hadronic decays from the resonance only ( $N_{had,1S}^{obs}$ ). The  $q\bar{q}$  vacuum polarization contribution to the total number of observed hadronic events can be calculated using  $R$  and  $B_{\mu\mu}(1S)$ , expressed in terms of the total number of  $\Upsilon(1S)$  decays  $N_{all,1S}$  ( $\equiv N_{had,1S}/(1 - 3B_{\mu\mu})$ ):

$$N_{q\bar{q},1S}^{obs} = N_{all,1S} \times RB_{\mu\mu,(1S)}\epsilon_{q\bar{q},1S},$$

or, in terms of  $N_{had,1S}^{obs}$ :

$$N_{q\bar{q},1S}^{obs} = (N_{had,1S}^{obs}/(\bar{\epsilon}_{had}(1 - 3B_{\mu\mu,1S}))) \times RB_{\mu\mu,1S}\epsilon_{q\bar{q},1S}.$$

Similarly, the number of direct photon events contributing to the hadronic event sample (independent of whether a high-energy photon is observed in the event; the number  $N_{\gamma gg,\gamma}$  corresponding to the hadronic events containing a high-energy photon is obtained independently by the model-dependent fits to the background-subtracted photon spectra)  $N_{\gamma gg,had}^{obs} = N_{had,1S}^{obs}/(\bar{\epsilon}_{had}(1 - 3B_{\mu\mu,1S})) \times B_{\gamma gg,1S}\epsilon_{\gamma gg,had}$ .

Using Monte-Carlo derived efficiencies for  $\epsilon_{q\bar{q},1S}$  and  $\epsilon_{\gamma gg, had}$  as well as the average hadronic event selection efficiency  $\bar{\epsilon}_{had}$  ( $\equiv f_{ggg}\epsilon_{ggg} + f_{gg\gamma}\epsilon_{gg\gamma} + f_{q\bar{q}}\epsilon_{q\bar{q}}$ , with  $f_{ggg}$ ,  $f_{gg\gamma}$  and  $f_{q\bar{q}}$  the fraction of true hadronic decays of the  $\Upsilon(1S)$  into the  $ggg$ ,  $gg\gamma$  and  $q\bar{q}$  final states, respectively),  $N_{all,1S}$  can be calculated, and the true number of resonant three-gluon events  $N_{ggg,1S} = N_{all,1S}(1 - N_{q\bar{q}}/N_{all,1S} - N_{\gamma gg}/N_{all,1S})$  then directly extracted. Note that, although the procedure seems circular, in that we must assume a value of  $B_{\gamma gg}$  at the outset, an error of 25% in  $B_{\gamma gg}$  corresponds to an error of only  $\sim 0.3\%$  in  $N_{ggg,1S}$ .

### Calculation of $R_\gamma$ in tagged $\Upsilon(2S) \rightarrow \pi\pi(1S)$ , $\Upsilon(1S) \rightarrow \gamma gg$ events

Following similar notation as presented above, we define  $N_{\pi\pi(1S)}^{obs}$  as the total (inclusive) observed number of  $\Upsilon(2S) \rightarrow \pi^+\pi^-\Upsilon(1S)$  events passing our hadronic event selection criteria:  $N_{\pi\pi(1S)}^{obs} = N_{\pi\pi(1S \rightarrow l+l^-)}\epsilon'_{\pi\pi(1S \rightarrow l+l^-)} + N_{\pi\pi(1S \rightarrow q\bar{q})}\epsilon'_{\pi\pi(1S \rightarrow q\bar{q})} + N_{\pi\pi(1S \rightarrow gg\gamma)}\epsilon'_{\pi\pi(1S \rightarrow gg\gamma)} + N_{\pi\pi(1S \rightarrow ggg)}\epsilon'_{\pi\pi(1S \rightarrow ggg)}$ , where all of the efficiencies are the conditional efficiencies, given that the two transition charged pions have been found. The explicit lepton veto suppresses contributions from dileptonic decays of the  $\Upsilon(1S)$ , and we again neglect these from further consideration. The number of observed hadronic events into a particular channel  $X$  is  $N_{\pi\pi(1S \rightarrow X)}^{obs} = N_{all,2S}B_{2S \rightarrow \pi\pi 1S}\epsilon_{2S \rightarrow \pi\pi 1S}B_{1S \rightarrow X}\epsilon'_{\pi\pi(1S \rightarrow X)}$ , related to the number of true events for that process by:  $N_{\pi\pi(1S \rightarrow X)} = N_{\pi\pi(1S \rightarrow X)}^{obs}/\epsilon'_{\pi\pi(1S \rightarrow X)}$ . So, for  $X$  corresponding to all hadronic final states,  $N_{\pi\pi(1S \rightarrow had)} = N_{\pi\pi(1S \rightarrow had)}^{obs}/(\bar{\epsilon}'_{had})(1 - 3B_{\mu\mu,1S})$ . Explicit evaluation of  $\epsilon'_{\pi\pi(1S \rightarrow \gamma gg)}$ ,  $\epsilon'_{\pi\pi(1S \rightarrow ggg)}$ , and  $\epsilon'_{\pi\pi(1S \rightarrow q\bar{q})}$ , and the average efficiency for an hadronic event to pass the event selection  $\bar{\epsilon}'_{had}$  is performed with Monte Carlo simulations of those cascade processes. The ratio:  $N_{\pi\pi(1S \rightarrow gg\gamma)}/N_{\pi\pi(1S \rightarrow had)}$  is now calculated directly (the numerator here is the number of efficiency-corrected dipion transition events which contain a high-energy photon) and the ratio  $R_\gamma$  extracted.

### Calculation of $\Upsilon(2S) \rightarrow ggg$ and Cascade Subtraction

For  $\Upsilon(2S)$  decays, a subtraction of the  $\Upsilon(1S) \rightarrow \gamma gg$  spectrum must be performed to isolate the  $\Upsilon(2S) \rightarrow \gamma gg$  component. Note that the methodology of this subtraction is checked, to some extent, by comparing our calculated, background-photon and cascade-subtracted Monte Carlo spectrum with the known input spectrum, as described in the text. The modification to the equations for the extraction of  $N_{ggg,1S}$  (as above) is straightforward. After subtracting the below- $\Upsilon(2S)$  continuum contribution to the spectrum spectrum, we have:

$$N_{had,total}^{obs}(ECM = 10.02) = N_{ggg,2S}\epsilon_{ggg,2S} + N_{gg\gamma,2S}\epsilon_{gg\gamma,2S} + N_{q\bar{q},2S}\epsilon_{q\bar{q},2S} + N_{\chi_b(J=0)}\epsilon_{\chi_b(J=0)} + N_{\chi_b(J=1)}\epsilon_{\chi_b(J=1)} + N_{\chi_b(J=2)}\epsilon_{\chi_b(J=2)} + N_{ggg,1S}\epsilon''_{ggg,1S} + N_{gg\gamma,1S}\epsilon''_{gg\gamma,1S} + N_{q\bar{q},1S}\epsilon''_{q\bar{q},1S} + N_{l+l^-,1S}\epsilon''_{l+l^-,1S},$$

with  $N_{q\bar{q},2S}\epsilon_{q\bar{q},2S} = N_{q\bar{q},2S}^{obs}$ , e.g. Note that  $\epsilon_{\chi_b}$  includes only hadronic decays of the  $\chi_b$  and explicitly excludes radiative transitions to the  $\Upsilon(1S)$ ; the latter are considered to contribute to the last three terms on the right-hand-side. We specify primed efficiencies ( $\epsilon''_{ggg,1S}$ , e.g.) again, as distinct (and generally higher, due to the slightly higher final state multiplicity due to contributions from transition charged pions) from the unprimed efficiencies presented previously. As before, knowing the fraction of inclusive resonant  $\Upsilon(2S)$  decays which decay

into hadronic final states (summing over all cascades into hadronic final states), we can derive the total number of  $\Upsilon(2S)$  decays via:  $N_{all,2S} = N_{had,2S}^{obs}/(\bar{\epsilon}_{had,2S}(1 - 3B_{\mu\mu,2S} - B(\Upsilon(2S) \rightarrow \Upsilon(1S)X) \times 3B_{\mu\mu,1S}))$ , again assuming that  $\Upsilon(2S) \rightarrow l^+l^-$  and  $\Upsilon(2S) \rightarrow \Upsilon(1S)X$ ;  $\Upsilon(1S) \rightarrow l^+l^-$  are explicitly removed by our lepton rejection, and that  $\epsilon_{had,2S}$  sums over all possible hadronic final states (including cascades).

Given  $N_{all,2S}$ , all contributions with the exception of  $N_{ggg,2S}$  and  $N_{gg\gamma,2S}$  are now explicitly calculated using Monte-Carlo derived efficiencies and known branching fractions via:

- $N_{q\bar{q},2S}^{obs} = N_{all,2S} R B_{\mu\mu,2S} \epsilon_{q\bar{q},2S}$
- $N_{\chi_b(J=0)}^{obs} = N_{all,2S} B_{\Upsilon(2S) \rightarrow \chi_b(J=0)} B_{\chi_b(J=2) \rightarrow gg} \epsilon_{\chi_b(J=0)}$
- $N_{\chi_b(J=1)}^{obs} = N_{all,2S} B_{\Upsilon(2S) \rightarrow \chi_b(J=1)} B_{\chi_b(J=1) \rightarrow q\bar{q}g} \epsilon_{\chi_b(J=1)}$
- $N_{\chi_b(J=2)}^{obs} = N_{all,2S} B_{\Upsilon(2S) \rightarrow \chi_b(J=2)} B_{\chi_b(J=0) \rightarrow gg} \epsilon_{\chi_b(J=2)}$
- $N_{ggg,1S}^{obs} = N_{all,2S} \epsilon_{\Upsilon(2S) \rightarrow \Upsilon(1S)X} B_{\Upsilon(2S) \rightarrow \Upsilon(1S)X} B_{\Upsilon(1S) \rightarrow ggg} \epsilon_{ggg,1S}''$
- $N_{q\bar{q},1S}^{obs} = N_{all,2S} \epsilon_{\Upsilon(2S) \rightarrow \Upsilon(1S)X} B_{\Upsilon(2S) \rightarrow \Upsilon(1S)X} R B_{\mu\mu,1S} \epsilon_{q\bar{q},1S}''$
- $N_{gg\gamma,1S}^{obs} = N_{all,2S} \epsilon_{\Upsilon(2S) \rightarrow \Upsilon(1S)X} B_{\Upsilon(2S) \rightarrow \Upsilon(1S)X} B_{\Upsilon(1S) \rightarrow gg\gamma} \epsilon_{gg\gamma,1S}''$

Thus, the cascade subtraction (last line) is immediately calculable in magnitude. We use the measured inclusive  $\Upsilon(1S)$  photon spectrum, simply normalized by luminosity, to subtract both the cascade direct photon contribution, as well as the contribution from photons from hadronic decays of particles produced in  $\Upsilon(2S) \rightarrow \Upsilon(1S)+X$  events. The shape of the measured  $\Upsilon(1S) \rightarrow \gamma+X$  spectrum is used as a basis for this subtraction, but modified to include Lorentz-boost and Doppler smearing effects.

The  $\Upsilon(3S)$  analysis proceeds similarly, with the addition of the  $\Upsilon(2S)$  cascade subtraction. Again, we separate decays of the type  $\Upsilon(3S) \rightarrow \chi_b(l)X$ ;  $\chi_b(l) \rightarrow \text{hadrons}$  (direct) from  $\Upsilon(3S) \rightarrow \Upsilon(2S/1S)X$ ;  $\Upsilon(2S/1S) \rightarrow gg\gamma$ .

## Appendix II) Calculation of strong coupling constant

The decay width  $\Upsilon \rightarrow gg\gamma$  has been calculated by Lepage and Mackenzie [26] in terms of the energy involved in the decay process (ie,  $\alpha_s(E_{cm})$ , or  $\alpha_s(M_\Upsilon)$ ):

$$\frac{\Gamma(\Upsilon \rightarrow gg\gamma)}{\Gamma(\Upsilon \rightarrow \mu^+\mu^-)} = \frac{8(\pi^2 - 9)}{9\pi\alpha_{QED}} \alpha_s^2(M_\Upsilon) \left[ 1 + (3.7 \pm 0.4) \frac{\alpha_s(M_\Upsilon)}{\pi} \right]. \quad (6)$$

Sanghera [31] uses a straightforward method to rewrite this expression in terms of an arbitrary energy (eg, renormalization) scale  $\mu$ :

$$\frac{\Gamma(\Upsilon \rightarrow gg\gamma)}{\Gamma(\Upsilon \rightarrow \mu^+\mu^-)} = A_\gamma \left( \frac{\alpha_s(\mu)}{\pi} \right)^2 + A_\gamma \left( \frac{\alpha_s(\mu)}{\pi} \right)^3 \left[ 2\pi b_0 \ln \left( \frac{\mu^2}{M_\Upsilon^2} \right) + (3.7 \pm 0.4) \right] \quad (7)$$

Where  $A_\gamma = \frac{8\pi(\pi^2-9)}{9\alpha_{QED}}$ ,  $b_0 = (33 - 2n_f)/12\pi$ , and  $n_f$  is the number of light quark flavors which participate in the process ( $n_f = 4$  for  $\Upsilon(1S)$  decays).

Similarly, the decay width  $\Upsilon \rightarrow ggg$  has been calculated by Bardeen et al. [27] and expressed by Lepage et al. [1, 28] as:

$$\frac{\Gamma(\Upsilon \rightarrow ggg)}{\Gamma(\Upsilon \rightarrow \mu^+ \mu^-)} = \frac{10(\pi^2 - 9)}{81\pi e_b^2} \frac{\alpha_s^3(M_\Upsilon)}{\alpha_{QED}^2} \left[ 1 + \frac{\alpha_s(M_\Upsilon)}{\pi} [2.770(7)\beta_0 - 14.0(5)] + \dots \right] \quad (8)$$

Where  $\beta_0 = 11 - (\frac{2}{3})n_f$ , and  $e_b = -\frac{1}{3}$ , the charge of the b quark. Here again Sanghera [31] uses the same algebraic technique to rewrite this in terms of the renormalization scale:

$$\frac{\Gamma(\Upsilon \rightarrow ggg)}{\Gamma(\Upsilon \rightarrow \mu^+ \mu^-)} = A_g \left( \frac{\alpha_s(\mu)}{\pi} \right)^3 + A_g \left( \frac{\alpha_s(\mu)}{\pi} \right)^4 \left[ 3\pi b_0 \ln \left( \frac{\mu^2}{M_\Upsilon^2} \right) - \left( \frac{2}{3} \right) B_f n_f + B_i \right] \quad (9)$$

Where  $A_g = \frac{10\pi^2(\pi^2-9)}{81e_b^2} \frac{1}{\alpha_{QED}^2}$ ,  $B_f = 2.770 \pm 0.007$ , and  $B_i = 16.47 \pm 0.58$ .

Note that the scale dependent QCD equations (7) and (9) are finite order in  $\alpha_s$ . If these equations were solved to all orders, then they could in principle be used to determine  $R_\gamma$  independent of the renormalization scale. But since we are dealing with calculations that are finite order, the question of an appropriate scale value must be addressed.

The renormalization scale may be defined in terms of the center of mass energy of the process,  $\mu^2 = f_\mu E_{cm}^2$ , where  $f_\mu$  is some positive fraction. But QCD does not tell us *a priori* what  $f_\mu$  should be. One possibility would be to define  $\mu = E_{cm}$ ; that is  $f_\mu=1$ . A number of phenomenological prescriptions [1, 29–31] have been proposed in an attempt to “optimize” the scale. However, each of these prescriptions yields scale values which, in general, vary greatly with the experimental quantity being measured [31]. With little consensus for a standard optimization procedure, we have chosen  $f_\mu = 1$  to facilitate a calculation of  $\alpha_s$  at each of the  $\Upsilon$  resonance energies.

For the  $\Upsilon(1S)$  analysis, using  $\mu = M_{\Upsilon(1S)}$  we find for  $\alpha_s(M_{\Upsilon(1S)})$

$$\alpha_s(M_{\Upsilon(1S)}) = 0.1681 \pm 0.0004 \pm 0.0115 \pm 0.0070; \quad (10)$$

for the  $\Upsilon(2S)$  analysis, using  $\mu = M_{\Upsilon(2S)}$  we find for  $\alpha_s(M_{\Upsilon(2S)})$

$$\alpha_s(M_{\Upsilon(2S)}) = 0.140 \pm 0.001 \pm 0.018 \pm 0.006; \quad (11)$$

for the  $\Upsilon(3S)$  analysis, using  $\mu = M_{\Upsilon(3S)}$  we find for  $\alpha_s(M_{\Upsilon(3S)})$

$$\alpha_s(M_{\Upsilon(3S)}) = 0.164 \pm 0.001 \pm 0.017 \pm 0.001, \quad (12)$$

The errors are due to the statistical, systematic and model dependence. These calculations were obtained by finding the zeroes of the ratio of equation 7 and equation 9 given our measurement of  $R_\gamma$  for each  $\Upsilon$  resonance, the relative rate of  $N_{gg\gamma}/N_{ggg}$ . The errors were obtained by shifting our measurement of  $R_\gamma$  by  $\pm\sigma$  and extracting  $\alpha_s$  for each relevant error-shifted central value.

These results can then be extrapolated to  $\mu = M_Z$  using equation 13 [22] with  $\mu_0 = M_\Upsilon$  for each resonance. For this calculation, only the first three terms of the  $\beta$ -function were considered[3].

$$\log \frac{\mu^2}{\mu_0^2} = \int_{\alpha_s(\mu_0)}^{\alpha_s(\mu)} \frac{d\alpha}{\beta(\alpha)} \quad (13)$$



This calculation for the  $\Upsilon(1S)$ ,  $\Upsilon(2S)$  and  $\Upsilon(3S)$  resulted in the following measurements of  $\alpha_s^{M_Z, \Upsilon(nS)}$ ,

$$\alpha_s^{M_Z, \Upsilon(1S)} = 0.1093 \pm 0.0001 \pm 0.0048 \pm 0.0029, \quad (14)$$

$$\alpha_s^{M_Z, \Upsilon(2S)} = 0.0978 \pm 0.0005 \pm 0.0089 \pm 0.0029, \quad (15)$$

$$\alpha_s^{M_Z, \Upsilon(3S)} = 0.1088 \pm 0.0006 \pm 0.0075 \pm 0.0006, \quad (16)$$

For the  $\Upsilon(1S)$ , this result is in fair agreement with the average value of  $\alpha_s^{M_Z} = 0.119 \pm 0.006$  obtained from many variables studied at all the LEP experiments [22]. This result is also in good agreement with  $\alpha_s^{M_Z} = 0.112 \pm 0.003$  obtained from an analysis of structure functions in deep inelastic scattering [33] and with the previous CLEO measurement of  $\alpha_s^{M_Z, \Upsilon(1S)}$  [20]. For the  $\Upsilon(2S)$  and  $\Upsilon(3S)$  measurements, however, we stress caution in interpreting these results, as it is not entirely clear what procedure should be used to define the renormalization scale. The current PDG world average is  $\alpha_s^{M_Z} = 0.1187(20) \pm 0.017$ , with which we are consistent for all resonances.

As an alternative to the extraction method outlined above, the strong coupling constant  $\alpha_s$  can be written as a function of the QCD scale parameter  $\Lambda_{\overline{MS}}$ , defined in the modified minimal subtraction scheme (MMSS)[22]. Figure 19 presents the contour plot of  $\alpha_s(\Lambda_{\overline{MS}}, f_\mu)$ . Similarly, the ratio of eqns. (2) and (4) above can be used to eliminate  $\alpha_s$  and provide a relationship between  $R_\gamma$ ,  $\Lambda_{\overline{MS}}$ , and  $f_\mu$  (Figure 20).

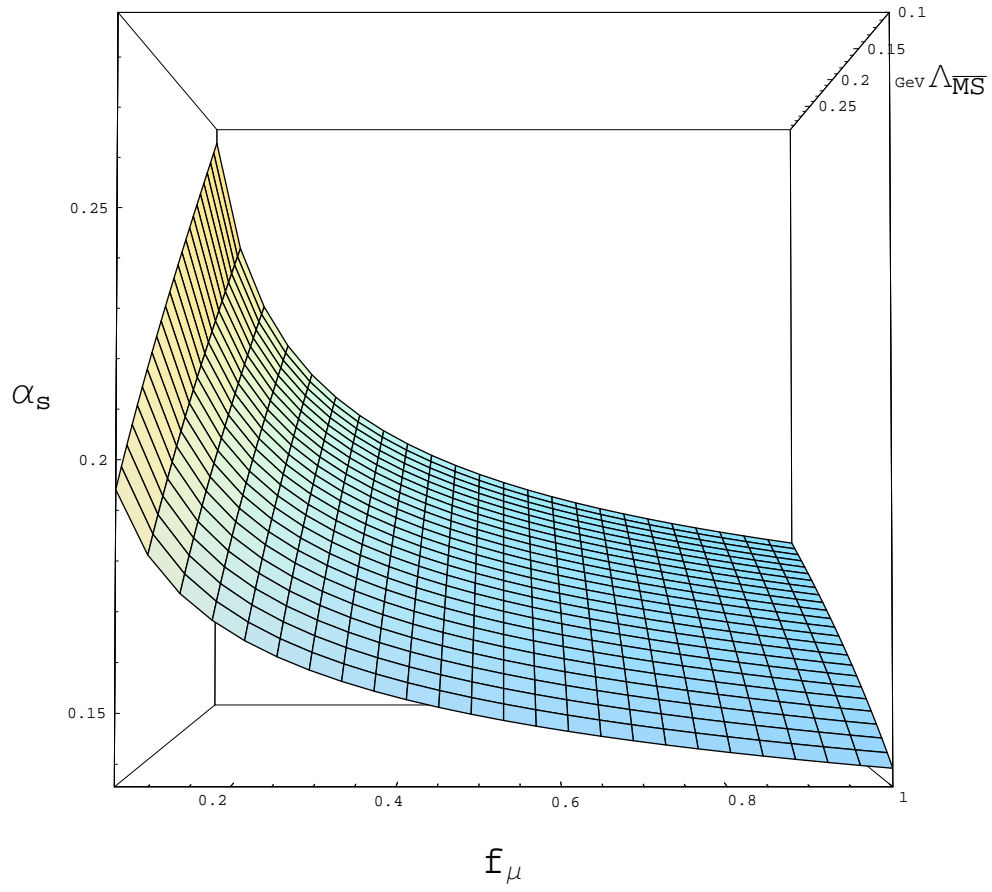


FIG. 19: Contour plot illustrating dependence of  $\alpha_s$  on the QCD scale parameter  $\Lambda_{\overline{MS}}$  and the momentum scale  $f_\mu$ .

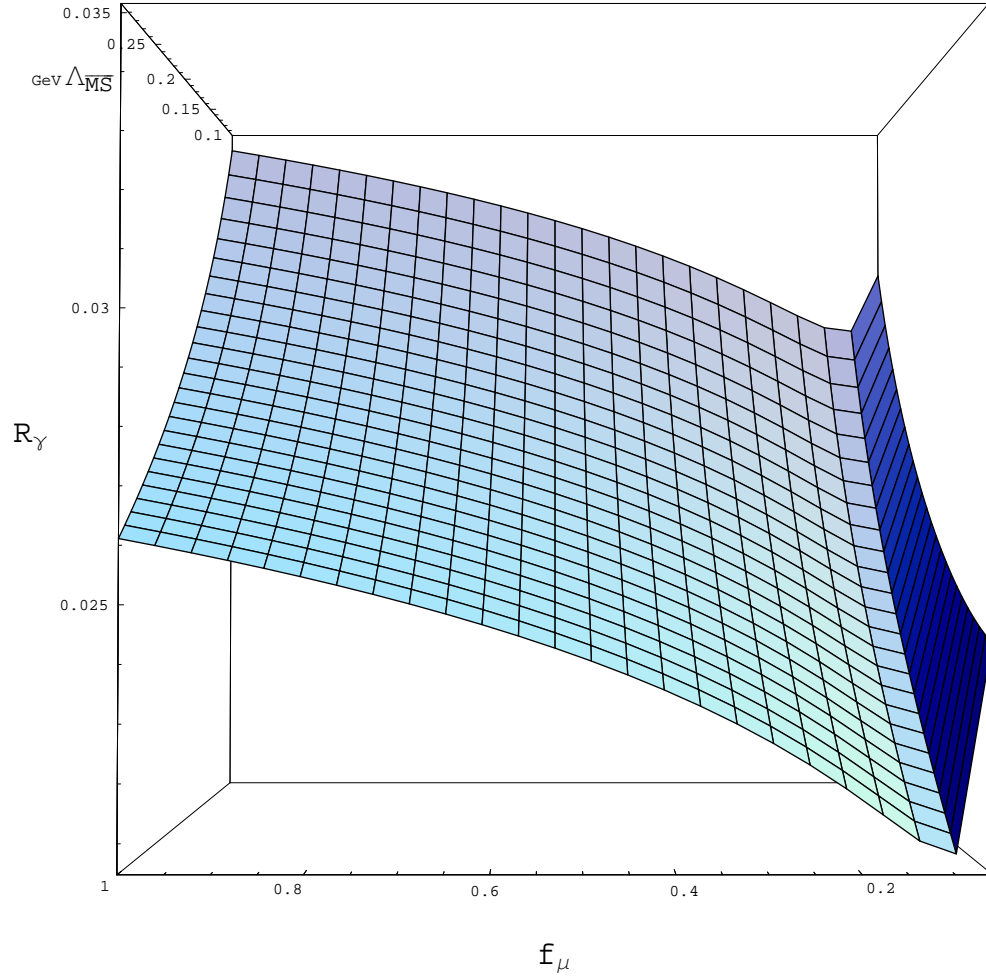


FIG. 20: Contour plot illustrating relationship between  $R_\gamma$ , the QCD scale parameter  $\Lambda_{\overline{MS}}$  and the momentum scale  $f_\mu$ .